

REDUCED BASIS METHOD FOR PARAMETRIZED ELLIPTIC ADVECTION–REACTION PROBLEMS*

Luca Dedè

*MOX–Modeling & Scientific Computing, Dipartimento di Matematica “F. Brioschi”,
Politecnico di Milano, P.zza Leonardo da Vinci 32, 20133, Milano, Italy
Email: luca.dede@polimi.it*

Abstract

In this work we consider the Reduced Basis method for the solution of parametrized advection–reaction partial differential equations. For the generation of the basis we adopt a stabilized finite element method and we define the Reduced Basis method in the “primal–dual” formulation for this stabilized problem. We provide a priori Reduced Basis error estimates and we discuss the effects of the finite element approximation on the Reduced Basis error. We propose an adaptive algorithm, based on the a posteriori Reduced Basis error estimate, for the selection of the sample sets upon which the basis are built; the idea leading this algorithm is the minimization of the computational costs associated with the solution of the Reduced Basis problem. Numerical tests demonstrate the efficiency, in terms of computational costs, of the “primal–dual” Reduced Basis approach with respect to an “only primal” one.

Mathematics subject classification: 35J25, 35L50, 65N15, 65N30, 76R99.

Key words: Parametrized advection–reaction partial differential equations, Reduced Basis method, “primal–dual” reduced basis approach, Stabilized finite element method, a posteriori error estimation.

1. Introduction

The Reduced Basis (RB) method is a computational approach which allows rapid and reliable predictions of functional outputs associated with the solution of Partial Differential Equations (PDEs) with parametric dependence [1, 6, 13–18]. Indeed, the RB method has a wide range of relevant applications in the characterization of engineering components or systems which require the prediction of certain “quantities of interest”, e.g., fluid dynamics, heat and mass transfer problems, (see, e.g., [11, 13, 20, 25, 27, 30]), as well as linear elasticity applications (see, e.g., [7, 12, 13, 26]) and many other physical problems (see, e.g., [3, 16, 18, 28]). Environmental problems represent a promising field of application for the RB method. Preliminary investigations have been made in [19, 21] for pollution problems in air, for which the RB method has been adopted to evaluate the concentration of pollutants emitted by industrial sites in certain zones of observation, such as cities [5], and to speed up the solution of the associated optimal control problems. Parametrized steady advection–diffusion PDEs have been used in this context with both geometrical and physical parameters, such as the location of industrial plants, the intensity or direction of the wind field and the diffusion coefficient.

* Received January 8, 2009 / Revised version received May 19, 2009 / Accepted June 26, 2009 /
Published online October 26, 2009 /

In this work we investigate the RB method for the evaluation of outputs, dependent on the solution of parametrized advection–reaction PDEs, in view of environmental applications, for which diffusion phenomena are negligible w.r.t. the transport and reaction ones.

The RB method is based on the decoupling of the generation and the projection stages of the approximation procedures, which leads to a decoupled offline–online computational approach. The complexity of the offline step, in which the basis are generated, depends on the dimension of the “truth” space, let say N_t , to which belongs the “truth” solution for a given parameter. The complexity of the online stage depends on the dimension of the RB space, let say N , with $N \ll N_t$, and on the parametric dependence.

For the definition of the “truth” space, we use the Finite Element (FE) method [23]. In order to get rid of the numerical instabilities due to the transport term of the hyperbolic advection–reaction PDE, we use the Streamline Diffusion Finite Element (SDFE) stabilized method [23, 31]. This leads to the transformation of the original hyperbolic PDE into a new one, with elliptic nature. We define the RB method for this parametrized stabilized advection–reaction problem, for which the affine decomposition property holds, and we consider the “primal–dual” RB approach [13,16,28], which requires the definition of a dual problem. This approach is well–suited both for the approximation and the error evaluation of the output and, as we highlight in this work, also for the reduction of the computational costs associated with the RB online step w.r.t. those of the “only primal” RB approach (without the dual problem). We provide a priori RB error estimates for both the solution and the output, thus highlighting the role of the FE approximation and stabilization in the RB method, being the total error composed by both the FE and RB ones. In particular, we show that, for the problem under consideration, the “complexity” of the RB approximation increases as the FE one improves by reducing the mesh size. We also report for this problem the a posteriori RB error estimate for the output according to [16,28]. We remark that the idea of using stabilized FE for the definition of the “truth” space has been already introduced in [19] for the solution of optimal control problems, even if a priori and a posteriori RB estimates and an error analysis for the FE and RB approximations have not been discussed. We use an adaptive algorithm for the definition of the RB basis, which is led by the a posteriori RB error estimate and based on a criterium of minimization of the online computational costs. Two numerical tests, inspired by environmental problems, are discussed; moreover, we experimentally show that the RB approximation is stable, if the FE one is stable.

This work is organized as follows. In Sec.2 we introduce the parametrized advection–reaction PDEs in an abstract setting and two problems with physical and geometrical parameters. In Sec.3 we provide the FE approximation of the parametrized problem, after having introduced the stabilization by means of the SDFE method; an a priori error analysis is reported for a particular case. Sec.4 deals with the RB method, for which the “primal–dual” RB approach is considered. Both a priori and a posteriori RB estimates are provided and the proposed adaptive algorithm for the choice of the sample sets is outlined. In Sec.5 we report some considerations about the numerical solution of the parametrized advection–reaction PDEs by means of the FE and RB methods. We discuss in Sec.6 two numerical tests. Concluding remarks follow.

2. Parametrized Advection–Reaction Equations

We introduce in an abstract setting the parametrized advection–reaction PDEs and we specify two problems with physical and geometrical parameters.

2.1. An abstract parametrized problem

Let us indicate with $\boldsymbol{\mu}$ the parameter vector, $\boldsymbol{\mu} \in \mathcal{D}$, with $\mathcal{D} \subset \mathbb{R}^P$ ($P \in \mathbb{N}$) the parameter set. We consider the following advection–reaction PDE:

$$\begin{cases} \mathbf{b}(\boldsymbol{\mu}) \cdot \nabla \phi(\boldsymbol{\mu}) + \sigma(\boldsymbol{\mu})\phi(\boldsymbol{\mu}) = f(\boldsymbol{\mu}) & \text{in } \Omega, \\ \phi(\boldsymbol{\mu}) = 0 & \text{on } \Gamma_D, \end{cases} \quad (2.1)$$

where $\Omega \subset \mathbb{R}^2$ is a bi–dimensional domain with boundary $\partial\Omega$. The parametrized advection field $\mathbf{b}(\boldsymbol{\mu}) \in [L^\infty(\Omega)]^2 \forall \boldsymbol{\mu} \in \mathcal{D}$ is chosen s.t.

$$\nabla \cdot \mathbf{b}(\boldsymbol{\mu}) = 0, \forall \boldsymbol{\mu} \in \mathcal{D},$$

the parametrized reaction term $\sigma(\boldsymbol{\mu}) \in L^\infty(\Omega) \forall \boldsymbol{\mu} \in \mathcal{D}$, s.t.

$$\sigma(\boldsymbol{\mu}) > 0, \forall \boldsymbol{\mu} \in \mathcal{D},$$

and the parametrized source term $f(\boldsymbol{\mu}) \in L^2(\Omega) \forall \boldsymbol{\mu} \in \mathcal{D}$. For the sake of simplicity, we have omitted to explicitly express the dependence of $\mathbf{b}(\boldsymbol{\mu})$, $\sigma(\boldsymbol{\mu})$ and $f(\boldsymbol{\mu})$ on the spatial coordinate $\mathbf{x} \in \mathbb{R}^2$, which should be read as $\mathbf{b}(\boldsymbol{\mu}, \mathbf{x})$, $\sigma(\boldsymbol{\mu}, \mathbf{x})$ and $f(\boldsymbol{\mu}, \mathbf{x})$, respectively. Moreover, we suppose that the parametrized data admit the *affine decomposition* property, e.g.:

$$\mathbf{b}(\boldsymbol{\mu}) = \mathbf{b}(\boldsymbol{\mu}, \mathbf{x}) = \left(\sum_{i=1}^{M_{b1}} \Theta_i^{b1}(\boldsymbol{\mu}) g_i^{b1}(\mathbf{x}), \sum_{j=1}^{M_{b2}} \Theta_j^{b2}(\boldsymbol{\mu}) g_j^{b2}(\mathbf{x}) \right),$$

with $\Theta_i^{b1}(\boldsymbol{\mu})$, $\Theta_j^{b2}(\boldsymbol{\mu}) \in C^0(\mathcal{D})$, $g_i^{b1}(\mathbf{x})$, $g_j^{b2}(\mathbf{x}) \in L^\infty(\Omega)$, $i = 1, \dots, M_{b1}$, $j = 1, \dots, M_{b2}$, for some M_{b1} , $M_{b2} \in \mathbb{N}$. In the same manner,

$$\sigma(\boldsymbol{\mu}) = \sigma(\boldsymbol{\mu}, \mathbf{x}) = \sum_{i=1}^{M_\sigma} \Theta_i^\sigma(\boldsymbol{\mu}) g_i^\sigma(\mathbf{x}),$$

with $\Theta_i^\sigma(\boldsymbol{\mu}) \in C^0(\mathcal{D})$ and $g_i^\sigma(\mathbf{x}) \in L^\infty(\Omega)$, $i = 1, \dots, M_\sigma$, for some $M_\sigma \in \mathbb{N}$; finally,

$$f(\boldsymbol{\mu}) = f(\boldsymbol{\mu}, \mathbf{x}) = \sum_{i=1}^{M_f} \Theta_i^f(\boldsymbol{\mu}) g_i^f(\mathbf{x}),$$

with $\Theta_i^f(\boldsymbol{\mu}) \in C^0(\mathcal{D})$ and $g_i^f(\mathbf{x}) \in L^2(\Omega)$, $i = 1, \dots, M_f$, for some $M_f \in \mathbb{N}$. We define the inflow boundary as

$$\Gamma_D(\boldsymbol{\mu}) := \{\mathbf{x} \in \partial\Omega : \mathbf{b}(\boldsymbol{\mu}) \cdot \hat{\mathbf{n}} < 0 \forall \boldsymbol{\mu} \in \mathcal{D}\},$$

where $\hat{\mathbf{n}}$ is the outward directed unit vector normal to $\partial\Omega$: we assume that $\Gamma_D(\boldsymbol{\mu})$ is “fixed”, in the sense that $\Gamma_D(\boldsymbol{\mu}) = \Gamma_D \forall \boldsymbol{\mu} \in \mathcal{D}$. Finally, we define the outflow boundary as $\Gamma_N := \partial\Omega \setminus \Gamma_D$.

The weak form of problem (2.1) reads:

$$\text{given } \boldsymbol{\mu} \in \mathcal{D}, \text{ find } \phi(\boldsymbol{\mu}) \in \mathcal{V} : \quad A(\phi(\boldsymbol{\mu}), v; \boldsymbol{\mu}) = F(v; \boldsymbol{\mu}) \quad \forall v \in \mathcal{V}, \quad (2.2)$$

where $\mathcal{V} := H_{\Gamma_D}^1(\Omega)$ is the usual Hilbert space of functions with null trace on Γ_D (see, e.g. [10]), and:

$$A(w, v; \boldsymbol{\mu}) := \int_{\Omega} (\mathbf{b}(\boldsymbol{\mu}) \cdot \nabla w v + \sigma(\boldsymbol{\mu}) w v) \, d\Omega, \quad F(v; \boldsymbol{\mu}) := \int_{\Omega} f(\boldsymbol{\mu}) v \, d\Omega. \quad (2.3)$$

Due to the affine decomposition assumptions made for $\mathbf{b}(\boldsymbol{\mu})$, $\sigma(\boldsymbol{\mu})$ and $f(\boldsymbol{\mu})$, the bilinear form $A(\cdot, \cdot; \boldsymbol{\mu})$ and the functional $F(\cdot; \boldsymbol{\mu})$ can be re-written as:

$$A(w, v; \boldsymbol{\mu}) = \sum_{q=1}^Q \vartheta_q(\boldsymbol{\mu}) A_q(w, v), \quad F(v; \boldsymbol{\mu}) = \sum_{q=1}^{Q^F} \vartheta_q^F(\boldsymbol{\mu}) F_q(v), \quad (2.4)$$

for some $Q \in \mathbb{N}$ and $Q^F \in \mathbb{N}$ with the bilinear forms $A_q(\cdot, \cdot)$ and the linear functionals $F_q(\cdot)$ not depending on $\boldsymbol{\mu}$.

Our goal consists in calculating an output $s(\boldsymbol{\mu})$ for some $\boldsymbol{\mu} \in \mathcal{D}$:

$$s(\boldsymbol{\mu}) = L(\phi(\boldsymbol{\mu}); \boldsymbol{\mu}), \quad (2.5)$$

where $L(\cdot; \boldsymbol{\mu})$ is a linear and continuous functional acting from \mathcal{V} to \mathbb{R} , s.t.:

$$L(v; \boldsymbol{\mu}) := \int_{\Omega} \gamma(\boldsymbol{\mu}) v \, d\Omega, \quad (2.6)$$

where $\gamma(\boldsymbol{\mu}) \in L^2(\Omega) \forall \boldsymbol{\mu} \in \mathcal{D}$ and subject to affine decomposition, s.t.:

$$s(\boldsymbol{\mu}) = \sum_{q=1}^{Q^L} \vartheta_q^L(\boldsymbol{\mu}) L_q(\phi(\boldsymbol{\mu})), \quad (2.7)$$

for some $Q^L \in \mathbb{N}$ and the linear functionals $L_q(\cdot)$ independent of $\boldsymbol{\mu}$.

2.2. Problem 1: physical parametrization

We consider a particular case, let say ‘‘Problem 1’’, of the general advection–reaction problem described in Sec. 2.1, with a physical parameter (see, e.g., also [19]).

We set $\boldsymbol{\mu} = \mu_p \in \mathcal{D} \subset \mathbb{R}$, with $\mu_p > 0$ a physical parameter which can be regarded as the magnitude of an advection field, whose direction is given by the unit vector $\mathbf{V} \in \mathbb{R}^2$. By referring to Eq. (2.1) we choose $\mathbf{b}(\mu_p) = \mu_p \mathbf{V}$, $\sigma(\mu_p) = 1$, $f(\mu_p) = g \in L^2(\Omega)$ and $\gamma(\mu_p) = \delta \in L^2(\Omega)$ (independent of μ_p). The corresponding advection–reaction problem reads:

$$\begin{cases} \mu_p \mathbf{V} \cdot \nabla \phi(\mu_p) + \phi(\mu_p) = g & \text{in } \Omega, \\ \phi(\mu_p) = 0 & \text{on } \Gamma_D, \end{cases} \quad (2.8)$$

for which the weak form (2.2) holds. In this case we have $Q = 2$, $Q^F = 1$ and $Q^L = 1$, with the functionals $F(v; \mu_p) = F(v)$ and $L(v; \mu_p) = L(v)$ both independent of μ_p .

2.3. Problem 2: physical and geometrical parametrization

We consider now a problem, let say ‘‘Problem 2’’, with both physical and geometrical parametric dependence, thus allowing to vary the shape of domain (see, e.g., [20, 24, 25, 27]).

Let us introduce a geometrical parameter μ_g , s.t. $\boldsymbol{\mu} = (\mu_p, \mu_g) \in \mathcal{D} \subset \mathbb{R}^2$, where μ_p is the physical parameter introduced in Sec. 2.2. We map the real domain into a reference domain, which is ‘‘fixed’’ as the μ_g varies, and we transform the original problem into a new one set on the reference domain.

By indicating with the subscript 0 the quantities defined on the real domain $\Omega_0 = \Omega_0(\mu_g)$, the parametrized advection–reaction PDE reads:

$$\begin{cases} \mu_p \mathbf{V}_0 \cdot \nabla_0 \phi_0(\boldsymbol{\mu}) + \phi_0(\boldsymbol{\mu}) = g_0 & \text{in } \Omega_0(\mu_g), \\ \phi_0(\boldsymbol{\mu}) = 0 & \text{on } \Gamma_{0D}(\mu_g), \end{cases} \quad (2.9)$$

with the same notation of Sec. 2.2. The problem on Ω_0 in weak form would read:

$$\text{given } \boldsymbol{\mu} \in \mathcal{D}, \text{ find } \phi_0(\boldsymbol{\mu}) \in \mathcal{V}_0 : A_0(\phi_0(\boldsymbol{\mu}), v; \boldsymbol{\mu}) = F_0(v; \boldsymbol{\mu}) \quad \forall v \in \mathcal{V}_0, \quad (2.10)$$

where $\mathcal{V}_0 := H_{\Gamma_{0D}}^1(\Omega_0(\mu_g))$; moreover,

$$s_0(\boldsymbol{\mu}) = \int_{\Omega_0(\mu_g)} \delta_0 \phi_0(\boldsymbol{\mu}) \, d\Omega_0(\mu_g).$$

Let us suppose that an *affine map*, acting from a reference domain Ω to the real domain $\Omega_0(\mu_g)$, could be provided and expressed in the following form:

$$\mathbf{x}_0 = T(\mu_g)\mathbf{x} + \mathbf{t}(\mu_g), \quad (2.11)$$

being the tensor $T(\mu_g) \in \mathbb{R}^{2 \times 2}$ and the vector $\mathbf{t}(\mu_g) \in \mathbb{R}^2$. In the case that the domains Ω_0 and Ω are partitioned into subdomains Ω_{0i} , Ω_i , s.t. $\cup_i \Omega_{0i} = \Omega_0$ and $\cup_i \Omega_i = \Omega$, it is necessary to define an affine map for each subdomain; for the sake of simplicity, we consider now non-partitioned domains, even if it is a straightforward matter to generalize to the case with subdomains.

By using the affine map, the weak problem (2.10) can be re-cast in the weak form (2.2), where $\mathcal{V} := H_{\Gamma_D}^1(\Omega)$ and $A(\cdot, \cdot; \boldsymbol{\mu})$, $F(\cdot; \boldsymbol{\mu})$ are defined in Eq. (2.3) and set on the reference domain Ω . By referring to Eq. (2.1) and by inspection of the weak form (2.2), we obtain:

$$\mathbf{b}(\boldsymbol{\mu}) = \mu_p \det(T(\mu_g)) T(\mu_g)^{-T} \mathbf{V}(\mu_g), \quad \sigma(\boldsymbol{\mu}) = \det(T(\mu_g)), \quad (2.12a)$$

$$f(\boldsymbol{\mu}) = \det(T(\mu_g)) g(\mu_g), \quad \gamma(\boldsymbol{\mu}) = \det(T(\mu_g)) \delta(\mu_g), \quad (2.12b)$$

where $\mathbf{V}(\mu_g) = V_0(T(\mu_g)\mathbf{x} + \mathbf{t}(\mu_g))$, $g(\mu_g) = g_0(T(\mu_g)\mathbf{x} + \mathbf{t}(\mu_g))$, $\delta(\mu_g) = \delta_0(T(\mu_g)\mathbf{x} + \mathbf{t}(\mu_g))$. Let us remark that we choose the affine map (2.11) such that the regularity hypothesis made in Sec. 2.1 hold for the coefficients in Eq. (2.12).

3. Finite Element Approximation: Stabilization

In this Section we consider the FE method for the numerical approximation of the hyperbolic advection–reaction PDE introduced in Sec. 2; with this aim, the SDFE method is introduced (see, e.g., [8, 9, 23, 31]). Moreover, we report an a priori FE error estimate and some estimates which will be used in Sec. 4.2 in view of the a priori RB error estimate.

3.1. Stabilization: the SDFE method

We introduce now the SDFE method for the numerical approximation of the abstract problem of Sec. 2.1, as proposed in [8] and discussed in [31].

Let us indicate with $\{K\}$ the triangular elements of a quasi-uniform unstructured mesh \mathcal{T}_h of the domain Ω , s.t. $\cup_{K \in \mathcal{T}_h} K = \overline{\Omega}$, and $h := \max_{K \in \mathcal{T}_h} \text{diam}(K)$. For the FE approximation we use piecewise linear basis functions $\forall K \in \mathcal{T}_h$ and we define the space $X_h := \{w \in C^0(\overline{\Omega}) : w|_K \in \mathbb{P}^1(K) \ \forall K \in \mathcal{T}_h\}$.

The stabilized discrete weak form of the problem (2.1) reads:

$$\text{given } \boldsymbol{\mu} \in \mathcal{D}, \text{ find } \phi_h(\boldsymbol{\mu}) \in \mathcal{V}_h : A_h(\phi_h(\boldsymbol{\mu}), v_h; \boldsymbol{\mu}) = F_h(v_h; \boldsymbol{\mu}) \quad \forall v_h \in \mathcal{V}_h, \quad (3.1)$$

where $\mathcal{V}_h \subset \mathcal{V}$ is the FE space, being $\mathcal{V}_h := \{w \in X_h : w(\mathbf{x}) = 0 \quad \forall \mathbf{x} \in \Gamma_D\}$, s.t. $N_h := \dim\{\mathcal{V}_h\} \equiv N_t$ represents the dimension of the “truth” space, and, from Eq. (2.3):

$$\begin{aligned} A_h(w, v; \boldsymbol{\mu}) &:= A(w, v; \boldsymbol{\mu}) + \varepsilon_h(h, \boldsymbol{\mu}) \int_{\Omega} \nabla w \cdot \nabla v \, d\Omega \\ &+ \delta_h(h, \boldsymbol{\mu}) \int_{\Omega} (\mathbf{b}(\boldsymbol{\mu}) \cdot \nabla w) (\mathbf{b}(\boldsymbol{\mu}) \cdot \nabla v) \, d\Omega + \delta_h(h, \boldsymbol{\mu}) \int_{\Omega} w \mathbf{b}(\boldsymbol{\mu}) \cdot \nabla v \, d\Omega, \end{aligned} \quad (3.2a)$$

$$F_h(v; \boldsymbol{\mu}) := F(v; \boldsymbol{\mu}) + \delta_h(h, \boldsymbol{\mu}) \int_{\Omega} f(\boldsymbol{\mu}) \mathbf{b}(\boldsymbol{\mu}) \cdot \nabla v \, d\Omega. \quad (3.2b)$$

Let us remark that the stabilized advection–reaction problem (3.1) corresponds now to an elliptic PDE.

The coefficients $\varepsilon_h(h, \boldsymbol{\mu})$ and $\delta_h(h, \boldsymbol{\mu})$ are chosen as in [8, 31]:

$$\varepsilon_h(h, \boldsymbol{\mu}) := C_\varepsilon(\boldsymbol{\mu})h^{3/2}, \quad \delta_h(h, \boldsymbol{\mu}) := C_\delta(\boldsymbol{\mu})h, \quad (3.3)$$

and are considered “small”. For example, due to dimensional reasons, for the Problems 1 and 2 of Sec.s 2.2 and 2.3, we choose $C_\varepsilon(\boldsymbol{\mu}) = c_\varepsilon \mu_p$ and $C_\delta(\boldsymbol{\mu}) = c_\delta / \mu_p$ for some $c_\varepsilon, c_\delta \in \mathbb{R}^+$.

Let us observe that the continuous stabilized version of the problem (3.1) would read:

$$\text{given } \boldsymbol{\mu} \in \mathcal{D}, \text{ find } \phi_c(\boldsymbol{\mu}) \in \mathcal{V} : A_h(\phi_c(\boldsymbol{\mu}), v_c; \boldsymbol{\mu}) = F_h(v_c; \boldsymbol{\mu}) \quad \forall v_c \in \mathcal{V}, \quad (3.4)$$

where the continuous solution $\phi_c(\boldsymbol{\mu}) \in \mathcal{V}$ of the stabilized problem differs from the continuous solution $\phi(\boldsymbol{\mu}) \in \mathcal{V}$ of the original problem in weak form (2.2).

The output corresponding to the FE solution is:

$$s_h(\boldsymbol{\mu}) := L(\phi_h(\boldsymbol{\mu}); \boldsymbol{\mu}). \quad (3.5)$$

Let us observe that, due to the affine decomposition assumptions made in Sec. 2.1 for $\mathbf{b}(\boldsymbol{\mu})$, $\sigma(\boldsymbol{\mu})$ and $f(\boldsymbol{\mu})$, even for the stabilized problem (see Eq. (2.4)), we have

$$A_h(w, v; \boldsymbol{\mu}) = \sum_{q=1}^{Q_h} \vartheta_{hq}(\boldsymbol{\mu}) A_{hq}(w, v), \quad F_h(v; \boldsymbol{\mu}) := \sum_{q=1}^{Q_h^F} \vartheta_{hq}^F(\boldsymbol{\mu}) F_{hq}(v); \quad (3.6)$$

for some $Q_h, Q_h^F \in \mathbb{N}$. By writing the FE solution as

$$\phi_h(\boldsymbol{\mu}) = \sum_{j=1}^{N_h} \phi_{hj}(\boldsymbol{\mu}) \varphi_j,$$

where φ_j is the FE Lagrangian basis function associated with the FE space \mathcal{V}_h , the FE solution is obtained from the following linear system:

$$\text{given } \boldsymbol{\mu} \in \mathcal{D}, \text{ find } \boldsymbol{\phi}_h(\boldsymbol{\mu}) \in \mathbb{R}^{N_h} : A_h(\boldsymbol{\mu}) \boldsymbol{\phi}_h(\boldsymbol{\mu}) = \mathbf{F}_h(\boldsymbol{\mu}), \quad (3.7)$$

where $(\boldsymbol{\phi}_h(\boldsymbol{\mu}))_i = \phi_{hi}(\boldsymbol{\mu})$; the matrix $A_h(\boldsymbol{\mu}) \in \mathbb{R}^{N_h \times N_h}$ and the vector $\mathbf{F}_h(\boldsymbol{\mu}) \in \mathbb{R}^{N_h}$ are defined respectively as

$$A_h(\boldsymbol{\mu}) := \sum_{q=1}^{Q_h} \vartheta_{hq}(\boldsymbol{\mu}) A_{hq} \quad \text{with} \quad (A_{hq})_{i,j} := A_{hq}(\varphi_i, \varphi_j)$$

and

$$\mathbf{F}_h(\boldsymbol{\mu}) := \sum_{q=1}^{Q_h^F} \vartheta_q^F(\boldsymbol{\mu}) \mathbf{F}_{hq} \quad \text{with} \quad (\mathbf{F}_{hq})_i := F_q(\varphi_i).$$

By recalling Eqs. (2.5), (2.7) and (3.5) and by defining the vector $\mathbf{L}_h(\boldsymbol{\mu}) \in \mathbb{R}^{N_h}$ as

$$\mathbf{L}_h(\boldsymbol{\mu}) := \sum_{q=1}^{Q^L} \vartheta_q^L(\boldsymbol{\mu}) \mathbf{L}_{hq} \quad \text{with} \quad (\mathbf{L}_{hq})_i := L_q(\varphi_i),$$

the output can finally be computed as

$$s_h(\boldsymbol{\mu}) = \phi_h(\boldsymbol{\mu}) \cdot \mathbf{L}_h(\boldsymbol{\mu}).$$

Let us now introduce the stabilized *dual problem* associated with the weak form (3.1) and the output (2.5):

$$\text{given } \boldsymbol{\mu} \in \mathcal{D}, \quad \text{find } \psi(\boldsymbol{\mu}) \in \mathcal{V} : \quad A_h(v, \psi(\boldsymbol{\mu}); \boldsymbol{\mu}) = -L(v; \boldsymbol{\mu}) \quad \forall v \in \mathcal{V} \quad (3.8)$$

and the corresponding discrete problem:

$$\text{given } \boldsymbol{\mu} \in \mathcal{D}, \quad \text{find } \psi_h(\boldsymbol{\mu}) \in \mathcal{V}_h : \quad A_h(v_h, \psi_h(\boldsymbol{\mu}); \boldsymbol{\mu}) = -L(v_h; \boldsymbol{\mu}) \quad \forall v_h \in \mathcal{V}_h. \quad (3.9)$$

For the sake of simplicity, we have avoided the subscript 'c' for $\psi(\boldsymbol{\mu}) \in \mathcal{V}$ in Eq. (3.8); we remark the fact that Eq. (3.8) does not represent the continuous dual problem, but only the continuous version of the stabilized one.

In analogy with the FE primal problem, the FE dual solution is obtained from the following linear system:

$$\text{given } \boldsymbol{\mu} \in \mathcal{D}, \quad \text{find } \boldsymbol{\psi}_h(\boldsymbol{\mu}) \in \mathbb{R}^{N_h} : \quad A_h(\boldsymbol{\mu})^T \boldsymbol{\psi}_h(\boldsymbol{\mu}) = -\mathbf{L}_h(\boldsymbol{\mu}), \quad (3.10)$$

where $(\boldsymbol{\psi}_h(\boldsymbol{\mu}))_i = \psi_{hi}(\boldsymbol{\mu})$, with $\psi_h(\boldsymbol{\mu}) = \sum_{j=1}^{N_h} \psi_{hj}(\boldsymbol{\mu}) \varphi_j$. In the same manner as the stabilized primal problem (3.1), also the dual one admits an affine decomposition, due to the assumption made for $\gamma(\boldsymbol{\mu})$ in Sec. 2.1.

Remark 3.1. Problem 3. Let us now introduce an advection–diffusion–reaction problem with a diffusion coefficient ε “small”, s.t. the solution of this elliptic problem assumes a hyperbolic behavior. Moreover, let us assume an homogeneous Dirichlet condition on the whole boundary $\partial\Omega$. The FE problem should be stabilized in order to avoid numerical instabilities. If we consider the SDFE method, the stabilized problem assumes the form (3.1), where the diffusion term ε has been neglected, being $\varepsilon \ll \varepsilon_h$ due to the hypothesis ε “small”. Moreover, let us observe that in this case we have $\mathcal{V}_h := \{w \in X_h : w(\mathbf{x}) = 0 \quad \forall \mathbf{x} \in \partial\Omega\}$. We will refer to this problem as Problem 3.

3.2. A priori FE error estimate

In this Section we consider the a priori FE error estimates associated with the solution of the stabilized problem (3.1) according to the SDFE method and the output. We provide the a priori FE error estimate for the Problem 3 of Remark 3.1; this allow us to make some considerations in Sec. 5 regarding the solution of stabilized advection–reaction problems by means of the FE and RB methods. Moreover, we report some estimates for the general stabilized problem of Sec. 3.1 in view of the a priori RB error estimate proposed in Sec. 4.2.

3.2.1. Problem 3

By referring to Problem 3 of Remark 3.1, we recall the a priori error estimates associated with the solution of the problem (3.1) and the corresponding output (3.5) (see [4, 31]).

Let us define the following norm, which depends on the parameter vector $\boldsymbol{\mu}$:

$$|||v|||^2 := \varepsilon_h(h, \boldsymbol{\mu}) \|\nabla v\|^2 + \delta_h(h, \boldsymbol{\mu}) \|\mathbf{b}(\boldsymbol{\mu}) \cdot \nabla v\|^2 + \|v\|^2, \quad (3.11)$$

where $\|\cdot\|$ indicates the usual $L^2(\Omega)$ norm ([10]). The stabilized Problem 3 admits an unique solution, being the form $A_h(\cdot, \cdot; \boldsymbol{\mu})$ bilinear, continuous and coercive and the functional $F_h(\cdot; \boldsymbol{\mu})$ linear and continuous. The continuity of the form $A_h(\cdot, \cdot; \boldsymbol{\mu})$ follows from:

$$\begin{aligned} |A_h(w_h, v_h; \boldsymbol{\mu})| &\leq \left[\max\{1, \|\sigma(\boldsymbol{\mu})\|_\infty\} + (\delta_h(h, \boldsymbol{\mu}))^{-1/2} \right] |||w_h||| |||v_h||| \\ &\quad \forall w_h, v_h \in \mathcal{V}_h, \quad \forall \boldsymbol{\mu} \in \mathcal{D}, \end{aligned} \quad (3.12)$$

while the coercivity from:

$$A_h(v_h, v_h; \boldsymbol{\mu}) \geq \alpha(\boldsymbol{\mu}) |||v_h|||^2 \quad \forall v_h \in \mathcal{V}_h, \quad \forall \boldsymbol{\mu} \in \mathcal{D}, \quad (3.13)$$

where $\alpha(\boldsymbol{\mu})$ is the coercivity constant:

$$\alpha(\boldsymbol{\mu}) := \min\{1, \|\sigma(\boldsymbol{\mu})\|_\infty\}. \quad (3.14)$$

For the sake of simplicity, $\|\sigma(\boldsymbol{\mu})\|_\infty$ stands for $\|\sigma(\boldsymbol{\mu})\|_{L^\infty(\Omega)}$. The same considerations hold also for the corresponding stabilized dual problem, which admits an unique solution.

The following a priori FE error estimates can be provided; see [4] and also [31] for the proof.

Proposition 3.1. *For Problem 3, by introducing the FE primal error $e_h^{pr}(\boldsymbol{\mu}) := \phi(\boldsymbol{\mu}) - \phi_h(\boldsymbol{\mu}) \in \mathcal{V}_h$ associated with the FE primal solution $\phi_h(\boldsymbol{\mu}) \in \mathcal{V}_h$ of Problem (3.1) and by assuming that the solution of problem (2.2) $\phi(\boldsymbol{\mu}) \in H^2(\Omega) \cap \mathcal{V} \forall \boldsymbol{\mu} \in \mathcal{D}$, the following a priori FE primal error estimate holds:*

$$|||e_h^{pr}(\boldsymbol{\mu})||| \leq C^{pr}(\boldsymbol{\mu}) h^{3/2} |\phi(\boldsymbol{\mu})|_{H^2(\Omega)} \quad \forall \boldsymbol{\mu} \in \mathcal{D}, \quad (3.15)$$

with $C^{pr}(\boldsymbol{\mu}) \in \mathbb{R}^+$ (see [4]) depending on $\boldsymbol{\mu}$, $\|\mathbf{b}(\boldsymbol{\mu})\|$ and $\|\sigma(\boldsymbol{\mu})\|_\infty$ and the seminorm $|\cdot|_{H^2(\Omega)}$ defined as

$$|w|_{H^2(\Omega)} := \left(\int_\Omega \left[\left(\frac{\partial^2 w}{\partial x^2} \right)^2 + \left(\frac{\partial^2 w}{\partial x \partial y} \right)^2 + \left(\frac{\partial^2 w}{\partial y^2} \right)^2 \right] d\Omega \right)^{1/2}$$

for some $w \in H^2(\Omega)$.

We notice that the estimate (3.15) shows the convergence rate 3/2 in h . If in particular we consider the Problem 1 endowed with the properties of Problem 3, then the estimate (3.15) reads ([4]):

$$|||e_h^{pr}(\mu_p)||| \leq c_{pr} \mu_p^{1/2} h^{3/2} |\phi(\mu_p)|_{H^2(\Omega)} \quad \forall \mu_p \in \mathcal{D}, \quad (3.16)$$

for some $c_{pr} \in \mathbb{R}^+$ which does not depend on μ_p .

Proposition 3.2. *For Problem 3, if the dual solution of problem (3.8) $\psi(\boldsymbol{\mu}) \in H^2(\Omega) \cap \mathcal{V} \forall \boldsymbol{\mu} \in \mathcal{D}$ and by introducing the FE dual error $e_h^{du}(\boldsymbol{\mu}) := \psi(\boldsymbol{\mu}) - \psi_h(\boldsymbol{\mu}) \in \mathcal{V}_h$, where $\psi_h(\boldsymbol{\mu}) \in \mathcal{V}_h$ is the FE dual solution of problem (3.9), the following a priori FE dual error estimate holds:*

$$|||e_h^{du}(\boldsymbol{\mu})||| \leq C^{du}(\boldsymbol{\mu}) h^{3/2} |\psi(\boldsymbol{\mu})|_{H^2(\Omega)} \quad \forall \boldsymbol{\mu} \in \mathcal{D}, \quad (3.17)$$

with $C^{du}(\boldsymbol{\mu}) \in \mathbb{R}^+$ (see [4]) depending on $\boldsymbol{\mu}$ and the data of the problem.

In view of the a priori FE error estimate for the output $s(\boldsymbol{\mu})$, we introduce the corrected (deflated) output:

$$\tilde{s}_h(\boldsymbol{\mu}) := s_h(\boldsymbol{\mu}) - \delta s_h(\boldsymbol{\mu}) \quad \text{with} \quad \delta s_h(\boldsymbol{\mu}) := -\varepsilon_h(h, \boldsymbol{\mu}) \int_{\Omega} \nabla \phi_h(\boldsymbol{\mu}) \cdot \nabla \psi_h \, d\Omega. \quad (3.18)$$

Proposition 3.3. *For the corrected output (3.18) associated with Problem 3, if $\phi(\boldsymbol{\mu}), \psi(\boldsymbol{\mu}) \in H^2(\Omega) \cap \mathcal{V} \forall \boldsymbol{\mu} \in \mathcal{D}$, the following a priori FE error estimate holds:*

$$|s(\boldsymbol{\mu}) - \tilde{s}_h(\boldsymbol{\mu})| \leq C^s(h, \boldsymbol{\mu}) h^{5/2} |\phi(\boldsymbol{\mu})|_{H^2(\Omega)} |\psi(\boldsymbol{\mu})|_{H^2(\Omega)} \quad \forall \boldsymbol{\mu} \in \mathcal{D}, \quad (3.19)$$

where the constant $C^s(h, \boldsymbol{\mu}) \in \mathbb{R}^+$ does not affect the convergence order in h , being

$$C^s(h, \boldsymbol{\mu}) := C_1^s(\boldsymbol{\mu}) \left\{ 1 + C_2^s(\boldsymbol{\mu}) h^{1/2} \right\},$$

with the constants $C_1^s(\boldsymbol{\mu})$ and $C_2^s(\boldsymbol{\mu})$ not dependent on h (see [4]).

In particular, for Problem 1 endowed with the properties of Problem 3 and for $h \rightarrow 0$, the estimate (3.19) reads ([4]):

$$|s(\mu_p) - \tilde{s}_h(\mu_p)| \leq c_s \mu_p^{3/2} h^{5/2} |\phi(\mu_p)|_{H^2(\Omega)} |\psi(\mu_p)|_{H^2(\Omega)} \quad \forall \mu_p \in \mathcal{D}, \quad (3.20)$$

for some $c_s \in \mathbb{R}^+$ which does not depend neither on h nor on μ_p .

3.2.2. The general case

We return now to the general stabilized problem of Sec. 3.1; we observe that in this case it is not straightforward to provide a priori FE error estimates as for Problem 3, being $\Gamma_D \neq \partial\Omega$.

However, we highlight some estimates in view of the analysis of the RB problem. We introduce the following norm:

$$\begin{aligned} \|v\|^2 := & \varepsilon_h(h, \boldsymbol{\mu}) \|\nabla v\|^2 + \delta_h(h, \boldsymbol{\mu}) \|\mathbf{b}(\boldsymbol{\mu}) \cdot \nabla v\|^2 + \|v\|^2 \\ & + \frac{1 + \delta_h(h, \boldsymbol{\mu})}{2} \|(\mathbf{b}(\boldsymbol{\mu}) \cdot \hat{\mathbf{n}})^{1/2} v\|_{\Gamma_N}^2, \end{aligned} \quad (3.21)$$

where $\|\cdot\|_{\Gamma_N} := \|\cdot\|_{L^2(\Gamma_N)}$; the norm (3.11) is a particular case of the norm (3.21) for $\Gamma_N \equiv \emptyset$. In analogy with Problem 3, it is simple to prove the existence and uniqueness of the solution of the problem (3.1); in fact, the form (3.2) is coercive and continuous also with the new norm (see [4]), being:

$$|A_h(w_h, v_h; \boldsymbol{\mu})| \leq \left[2 \max\{1, \|\sigma(\boldsymbol{\mu})\|_{\infty}\} + (\delta_h(h, \boldsymbol{\mu}))^{-1/2} \right] \|w_h\| \|v_h\| \quad \forall \boldsymbol{\mu} \in \mathcal{D}. \quad (3.22)$$

Similarly, existence and uniqueness of the FE dual solution are ensured.

4. Reduced Basis Method

In this Section we consider the RB method for the solution of the stabilized parametrized advection–reaction problem of Sec. 3 according to the “primal–dual” RB approach. We provide both the a priori and a posteriori RB error estimates and an adaptive algorithm for the choice of the sample sets.

4.1. The RB method for the stabilized problem

We recall the RB method based on the “truth” stabilized problem of Sec. 3.1; in particular, we consider the “primal–dual” RB approach. For more details about the RB method and its applications, see, e.g., [6, 13, 16, 18, 20, 27, 30].

Let us introduce the following set of parameters $\mathcal{S}_N^{pr} := \{\boldsymbol{\mu}_1^{pr}, \dots, \boldsymbol{\mu}_{N^{pr}}^{pr}\}$, with $\boldsymbol{\mu}_i^{pr} \in \mathcal{D}$, $i = 1, \dots, N^{pr}$, $N^{pr} \in \mathbb{N}$; the superscript “pr” is used to refer to the primal problem. The set of parameters $\boldsymbol{\mu}_i^{pr}$ and their number N^{pr} will be chosen in \mathcal{D} according to the adaptive algorithm (see, Sec. 4.4). For each $\boldsymbol{\mu}_i^{pr} \in \mathcal{S}_N^{pr}$, we solve, by means of the FE element method, the stabilized primal problem (3.1), thus obtaining the corresponding discretized primal solutions $\phi_h(\boldsymbol{\mu}_i^{pr}) \in \mathcal{V}_h$. Then, we define the RB primal space:

$$\mathcal{V}_N^{pr} := \text{span} \{ \xi_i := \phi_h(\boldsymbol{\mu}_i^{pr}) \quad i = 1, \dots, N^{pr} \} \quad (4.1)$$

and the RB primal problem:

$$\text{given } \boldsymbol{\mu} \in \mathcal{D}, \quad \text{find } \phi_N(\boldsymbol{\mu}) \in \mathcal{V}_N^{pr} : A_h(\phi_N(\boldsymbol{\mu}), v_N; \boldsymbol{\mu}) = F_h(v_N; \boldsymbol{\mu}) \quad \forall v_N \in \mathcal{V}_N^{pr}, \quad (4.2)$$

where $A_h(\cdot, \cdot; \boldsymbol{\mu})$ and $F_h(\cdot; \boldsymbol{\mu})$ are defined in Eq.(3.2) and $\phi_N(\boldsymbol{\mu}) = \sum_{j=1}^{N^{pr}} \phi_{Nj}(\boldsymbol{\mu}) \xi_j$. For the sake of simplicity, we have used the notation $\phi_N(\boldsymbol{\mu})$ to indicate the RB solution $\phi_{hN}(\boldsymbol{\mu})$ of the RB primal problem (4.2).

Remark 4.1. In order to avoid ill–conditioning troubles with the solution of problem (4.2), we adopt an orthonormal basis for the generation of the RB space \mathcal{V}_N^{pr} ; in particular we consider the Gram–Schmidt orthonormalization w.r.t. the inner product (\cdot, \cdot) induced by the norm $\|\cdot\|$ (see, e.g., [16]). Let us indicate the new orthonormal basis for the RB space \mathcal{V}_N^{pr} as $\{\varrho_i\}_{i=1}^{N^{pr}}$, which we compute according to the following procedure:

$$\varrho_1 = \xi_1 / \|\xi_1\|; \quad z_i = \xi_i - \sum_{j=1}^{i-1} (\varrho_j, \xi_i) \varrho_j, \quad \varrho_i = z_i / \|z_i\|, \quad i = 2, \dots, N^{pr}. \quad (4.3)$$

We obtain that $\mathcal{V}_N^{pr} = \text{span}\{\xi_i, i = 1, \dots, N^{pr}\} = \text{span}\{\varrho_i, i = 1, \dots, N^{pr}\}$. Let us notice that, for the sake of simplicity, we will identify the basis $\{\xi_i\}_{i=1}^{N^{pr}}$ used in Eq.s (4.1) and (4.2) as the orthonormal basis $\{\varrho_i\}_{i=1}^{N^{pr}}$.

Owing to the affine decomposition hypothesis for $A_h(\cdot, \cdot; \boldsymbol{\mu})$ and $F_h(\cdot; \boldsymbol{\mu})$ (see Eq.(3.6)), Eq.(4.2) reads:

$$\begin{cases} \text{Given } \boldsymbol{\mu} \in \mathcal{D}, \quad \text{find } \phi_{Nj}(\boldsymbol{\mu}) \quad j = 1, \dots, N^{pr} : \\ \sum_{q=1}^{Q_h} \vartheta_{hq}(\boldsymbol{\mu}) A_{hq}(\xi_j, \xi_i) \phi_{Nj}(\boldsymbol{\mu}) = \sum_{q=1}^{Q_h^F} \vartheta_{hq}^F(\boldsymbol{\mu}) F_{hq}(\xi_i), \quad i = 1, \dots, N^{pr}. \end{cases} \quad (4.4)$$

which can be finally re–written in matricial notation as:

$$\text{given } \boldsymbol{\mu} \in \mathcal{D}, \quad \text{find } \boldsymbol{\phi}_N(\boldsymbol{\mu}) \in \mathbb{R}^{N^{pr}} : A_N^{pr}(\boldsymbol{\mu}) \boldsymbol{\phi}_N(\boldsymbol{\mu}) = \mathbf{F}_N^{pr}(\boldsymbol{\mu}), \quad (4.5)$$

where the matrix $A_N^{pr}(\boldsymbol{\mu}) \in \mathbb{R}^{N^{pr} \times N^{pr}}$ and the vector $\mathbf{F}_N^{pr}(\boldsymbol{\mu}) \in \mathbb{R}^{N^{pr}}$ are defined respectively as

$$A_N^{pr}(\boldsymbol{\mu}) := \sum_{q=1}^{Q_h} \vartheta_{hq}(\boldsymbol{\mu}) A_{Nq}^{pr} \quad \text{with} \quad (A_{Nq}^{pr})_{i,j} := A_{hq}(\xi_j, \xi_i)$$

and

$$\mathbf{F}_N^{pr}(\boldsymbol{\mu}) := \sum_{q=1}^{Q^F} \vartheta_{hq}^F(\boldsymbol{\mu}) \mathbf{F}_{Nq} \quad \text{with} \quad \left(\mathbf{F}_{Nq}^{pr} \right)_i := F_{hq}(\xi_i).$$

By recalling Eqs. (2.5) and (2.8), it follows that for some $\boldsymbol{\mu} \in \mathcal{D}$:

$$s_N(\boldsymbol{\mu}) := L(\phi_N(\boldsymbol{\mu}); \boldsymbol{\mu}) = \phi_N(\boldsymbol{\mu}) \cdot \mathbf{L}_N^{pr}(\boldsymbol{\mu}), \quad (4.6)$$

where $\mathbf{L}_N^{pr}(\boldsymbol{\mu}) \in \mathbb{R}^{N^{pr}}$ is defined as

$$\mathbf{L}_N^{pr}(\boldsymbol{\mu}) := \sum_{q=1}^{Q^L} \vartheta_q^L(\boldsymbol{\mu}) \mathbf{L}_{Nq}^{pr} \quad \text{with} \quad \left(\mathbf{L}_{Nq}^{pr} \right)_i := L_q(\xi_i).$$

By considering the RB dual problem, we select a set of parameters $\mathcal{S}_N^{du} := \{\boldsymbol{\mu}_1^{du}, \dots, \boldsymbol{\mu}_{N^{du}}^{du}\}$, with $\boldsymbol{\mu}_i^{du} \in \mathcal{D}$, $i = 1, \dots, N^{du}$, $N^{du} \in \mathbb{N}$; the superscript 'du' refers to the dual problem.

Remark 4.2. Let us observe that we consider the non-integrated primal and dual RB approach [16], for which, not only $N^{pr} \neq N^{du}$, but also the sets \mathcal{S}_N^{pr} and \mathcal{S}_N^{du} are composed by different parameters; this issue will be re-called and discussed in Sec.4.4.3.

By defining the RB dual space as:

$$\mathcal{V}_N^{du} := \text{span} \{ \zeta_i := \psi_h(\boldsymbol{\mu}_i^{du}) \quad i = 1, \dots, N^{du} \}, \quad (4.7)$$

where $\psi_h(\boldsymbol{\mu}_i^{du})$ is the solution of the FE dual problem (3.9) for $\boldsymbol{\mu} = \boldsymbol{\mu}_i^{du}$ and $\{\zeta_i\}_{i=1}^{N^{du}}$ is an orthonormal basis (see Remark 4.1), then the RB dual problem reads:

$$\text{given } \boldsymbol{\mu} \in \mathcal{D}, \quad \text{find } \psi_N(\boldsymbol{\mu}) \in \mathcal{V}_N^{du} : A_h(v_N, \psi_N(\boldsymbol{\mu}); \boldsymbol{\mu}) = -L(v_N; \boldsymbol{\mu}) \quad \forall v_N \in \mathcal{V}_N^{du}, \quad (4.8)$$

being RB dual solution

$$\psi_N(\boldsymbol{\mu}) = \sum_{j=1}^{N^{du}} \psi_{Nj}(\boldsymbol{\mu}) \zeta_j.$$

According to Eqs. (2.7), (3.6) and (3.9), Eq. (4.8) can be expressed in matricial notation as:

$$\text{given } \boldsymbol{\mu} \in \mathcal{D}, \quad \text{find } \boldsymbol{\psi}_N(\boldsymbol{\mu}) \in \mathbb{R}^{N^{du}} : A_N^{du}(\boldsymbol{\mu}) \boldsymbol{\psi}_N(\boldsymbol{\mu}) = -\mathbf{L}_N^{du}(\boldsymbol{\mu}), \quad (4.9)$$

where the matrix $A_N^{du}(\boldsymbol{\mu}) \in \mathbb{R}^{N^{du} \times N^{du}}$ and the vector $\mathbf{L}_N^{du}(\boldsymbol{\mu}) \in \mathbb{R}^{N^{du}}$ are defined as

$$A_N^{du}(\boldsymbol{\mu}) := \sum_{q=1}^{Q_h} \vartheta_{hq}(\boldsymbol{\mu}) A_{Nq}^{du} \quad \text{with} \quad (A_{Nq}^{du})_{i,j} := A_{hq}(\zeta_i, \zeta_j)$$

and

$$\mathbf{L}_N^{du}(\boldsymbol{\mu}) := \sum_{q=1}^{Q^L} \vartheta_q^L(\boldsymbol{\mu}) \mathbf{L}_{Nq} \quad \text{with} \quad (\mathbf{L}_{Nq}^{du})_i := L_q(\zeta_i).$$

4.2. A priori RB error estimate

We provide in the following Propositions the a priori RB error estimates both for the RB primal and dual solutions and the output.

Proposition 4.1. *By introducing the RB primal error $e_N^{pr}(\boldsymbol{\mu}) := \phi_h(\boldsymbol{\mu}) - \phi_N(\boldsymbol{\mu}) \in \mathcal{V}_h$, being $\phi_h(\boldsymbol{\mu}) \in \mathcal{V}_h$ and $\phi_N(\boldsymbol{\mu}) \in \mathcal{V}_N^{pr} \subset \mathcal{V}_h$ the FE and RB primal solutions of problems (3.1) and (4.2), respectively, the following a priori RB primal error estimate holds:*

$$\|e_N^{pr}(\boldsymbol{\mu})\| \leq \Xi(\boldsymbol{\mu}) \inf_{v_N \in \mathcal{V}_N^{pr}} \|\phi_h(\boldsymbol{\mu}) - v_N\| \quad \forall \boldsymbol{\mu} \in \mathcal{D}, \quad (4.10)$$

where

$$\Xi(\boldsymbol{\mu}) := \frac{2 \max\{1, \|\sigma(\boldsymbol{\mu})\|_\infty\} + (C_\delta(\boldsymbol{\mu})h)^{-1/2}}{\min\{1, \|\sigma(\boldsymbol{\mu})\|_\infty\}}, \quad (4.11)$$

$C_\delta(\boldsymbol{\mu})$ is defined in Eq. (3.3) and the same notation of Sec. 3.2 is used.

Proof. From the coercivity property (3.13) of $A_h(\cdot, \cdot; \boldsymbol{\mu})$ w.r.t. the norm $\|\cdot\|$ of Eq. (3.21) (or Eq. (3.11) for Problem 3), it follows:

$$\|e_N^{pr}(\boldsymbol{\mu})\|^2 \leq \frac{1}{\min\{1, \|\sigma(\boldsymbol{\mu})\|_\infty\}} A_h(e_N^{pr}(\boldsymbol{\mu}), e_N^{pr}(\boldsymbol{\mu}); \boldsymbol{\mu}) \quad \forall \boldsymbol{\mu} \in \mathcal{D}. \quad (4.12)$$

By observing from Eqs. (3.1) and (4.2) that, for the RB primal problem, the Galerkin orthogonality property holds $A_h(e_N^{pr}(\boldsymbol{\mu}), v_N; \boldsymbol{\mu}) = 0 \forall v_N \in \mathcal{V}_N^{pr}$, the bilinear form $A_h(e_N^{pr}(\boldsymbol{\mu}), e_N^{pr}(\boldsymbol{\mu}); \boldsymbol{\mu})$ can be written as:

$$A_h(e_N^{pr}(\boldsymbol{\mu}), e_N^{pr}(\boldsymbol{\mu}); \boldsymbol{\mu}) = A_h(e_N^{pr}(\boldsymbol{\mu}), \phi_h(\boldsymbol{\mu}) - v_N; \boldsymbol{\mu}) \quad \forall v_N \in \mathcal{V}_N^{pr}, \quad (4.13)$$

being $\phi_h(\boldsymbol{\mu}) - v_N \in \mathcal{V}_N^{pr}$. By applying the inequality (3.22) to Eq. (4.13), recalling Eq. (4.12) and simplifying the term $\|e_N^{pr}(\boldsymbol{\mu})\|$ both on the l.h.s and r.h.s of the inequality, we have:

$$\|e_N^{pr}(\boldsymbol{\mu})\| \leq \frac{2 \max\{1, \|\sigma(\boldsymbol{\mu})\|_\infty\} + (\delta_h(h, \boldsymbol{\mu}))^{-1/2}}{\min\{1, \|\sigma(\boldsymbol{\mu})\|_\infty\}} \|\phi_h(\boldsymbol{\mu}) - v_N\|, \quad \forall v_N \in \mathcal{V}_N^{pr}, \quad \forall \boldsymbol{\mu} \in \mathcal{D}. \quad (4.14)$$

Then, from Eqs. (4.14) and (3.3) the result (4.10) follows. \square

Let us observe that for Problem 1, the estimate (4.10) holds with the constant (4.11):

$$\Xi(\boldsymbol{\mu}_p) = 2 + \left(\frac{\mu_p}{c_\delta h} \right)^{1/2}. \quad (4.15)$$

Proposition 4.2. *By defining the RB dual error $e_N^{du}(\boldsymbol{\mu}) := \psi_h(\boldsymbol{\mu}) - \psi_N(\boldsymbol{\mu}) \in \mathcal{V}_h$, with $\psi_h(\boldsymbol{\mu}) \in \mathcal{V}_h$ and $\psi_N(\boldsymbol{\mu}) \in \mathcal{V}_N^{du} \subset \mathcal{V}_h$ the FE and RB dual solutions of problems (3.9) and (4.8), respectively, the following a priori RB dual error estimate holds:*

$$\|e_N^{du}(\boldsymbol{\mu})\| \leq \Xi(\boldsymbol{\mu}) \inf_{v_N \in \mathcal{V}_N^{du}} \|\psi_h(\boldsymbol{\mu}) - v_N\| \quad \forall \boldsymbol{\mu} \in \mathcal{D}, \quad (4.16)$$

where $\Xi(\boldsymbol{\mu})$ is defined in Eq. (4.11).

Proof. The desired result (4.16) is obtained mimicking the proof of Proposition 4.1 for the dual problem. \square

Proposition 4.3. *For the RB output $s_N(\boldsymbol{\mu})$ (4.6), the following a priori RB output error estimate holds w.r.t. the FE output $s_h(\boldsymbol{\mu})$ (3.5):*

$$|s_h(\boldsymbol{\mu}) - s_N(\boldsymbol{\mu})| \leq \Xi(\boldsymbol{\mu})^3 \left(\inf_{v_N \in \mathcal{V}_N^{pr}} \|\phi_h(\boldsymbol{\mu}) - v_N\| \right) \left(\inf_{w_N \in \mathcal{V}_N^{du}} \|\psi_h(\boldsymbol{\mu}) - w_N\| \right), \quad \forall \boldsymbol{\mu} \in \mathcal{D}, \quad (4.17)$$

where $\Xi(\boldsymbol{\mu})$ is defined in Eq. (4.11).

Proof. From Eq.s (2.5), (3.5), (3.9) and (4.6) and the Galerkin orthogonality property, we have:

$$s_h(\boldsymbol{\mu}) - s_N(\boldsymbol{\mu}) = L(e_N^{pr}(\boldsymbol{\mu}); \boldsymbol{\mu}) = -A_h(e_N^{pr}(\boldsymbol{\mu}), e_N^{du}(\boldsymbol{\mu}); \boldsymbol{\mu}), \quad (4.18)$$

which, according to the inequality (3.22), leads to the desired result (4.17). \square

4.3. A posteriori RB error estimate

In this section we discuss the a posteriori RB error estimate for the output; for further details and the proof of Proposition 4.4 we refer the reader to [28] and also to [13, 16].

Let us define the RB residuals associated with the RB primal and dual problems by recalling respectively Eqs. (3.1) and (3.9):

$$R_N^{pr}(v_h; \boldsymbol{\mu}) := F_h(v_h; \boldsymbol{\mu}) - A_h(\phi_N(\boldsymbol{\mu}), v_h; \boldsymbol{\mu}) = A_h(e_N^{pr}(\boldsymbol{\mu}), v_h; \boldsymbol{\mu}), \quad (4.19)$$

$$R_N^{du}(v_h; \boldsymbol{\mu}) := -L(v_h; \boldsymbol{\mu}) - A_h(v_h, \psi_N(\boldsymbol{\mu}); \boldsymbol{\mu}) = A_h(v_h, e_N^{du}(\boldsymbol{\mu}); \boldsymbol{\mu}), \quad (4.20)$$

with $v_h \in \mathcal{V}_h$. Moreover, we define the corrected RB output (deflated) [28]:

$$\tilde{s}_N(\boldsymbol{\mu}) := s_N(\boldsymbol{\mu}) - R_N^{pr}(\psi_N(\boldsymbol{\mu}); \boldsymbol{\mu}) \quad (4.21)$$

and we express the error w.r.t. the corrected RB output as:

$$s_h(\boldsymbol{\mu}) - \tilde{s}_N(\boldsymbol{\mu}) = -R_N^{pr}(e_N^{du}(\boldsymbol{\mu}); \boldsymbol{\mu}). \quad (4.22)$$

Then, we introduce the dual norm of $\|\cdot\|$ (see, e.g., [10]), indicated as $\|\cdot\|_*$, from which we have:

$$\|R_N^{pr}(\cdot; \boldsymbol{\mu})\|_* := \sup_{v_h \in \mathcal{V}_h \setminus \{0\}} \frac{R_N^{pr}(v_h; \boldsymbol{\mu})}{\|v_h\|} \quad \forall \boldsymbol{\mu} \in \mathcal{D} \quad (4.23)$$

and similarly for the dual residual $R_N^{du}(\cdot; \boldsymbol{\mu})$. Finally, we introduce the parametrized Babuška *inf-sup* stability constant (see [2]) $\beta(\boldsymbol{\mu})$:

$$\beta(\boldsymbol{\mu}) := \inf_{w_h \in \mathcal{V}_h \setminus \{0\}} \sup_{v_h \in \mathcal{V}_h \setminus \{0\}} \frac{A_h(w_h, v_h; \boldsymbol{\mu})}{\|w_h\| \|v_h\|} \quad \forall \boldsymbol{\mu} \in \mathcal{D}. \quad (4.24)$$

We notice that, being the bilinear form $A_h(\cdot, \cdot; \boldsymbol{\mu})$ (3.2) coercive (Eq. (3.13)), the parametrized *inf-sup* constant (4.24) is positive $\beta(\boldsymbol{\mu}) > 0 \forall \boldsymbol{\mu} \in \mathcal{D}$.

Proposition 4.4. *For the RB corrected output $\tilde{s}_N(\boldsymbol{\mu})$ (4.21) the following a posteriori RB output error estimate holds:*

$$|s_h(\boldsymbol{\mu}) - \tilde{s}_N(\boldsymbol{\mu})| \leq \Delta_N^s(\boldsymbol{\mu}) \quad \forall \boldsymbol{\mu} \in \mathcal{D}, \quad (4.25)$$

where $\Delta_N^s(\boldsymbol{\mu}) := \Delta_N^{pr}(\boldsymbol{\mu}) \Delta_N^{du}(\boldsymbol{\mu})$, with:

$$\Delta_N^{pr}(\boldsymbol{\mu}) := \frac{1}{\sqrt{\beta(\boldsymbol{\mu})}} \|\| R_N^{pr}(\cdot; \boldsymbol{\mu}) \|\|_*, \quad \Delta_N^{du}(\boldsymbol{\mu}) := \frac{1}{\sqrt{\beta(\boldsymbol{\mu})}} \|\| R_N^{du}(\cdot; \boldsymbol{\mu}) \|\|_*, \quad (4.26)$$

being the RB primal and dual residuals defined in Eqs. (4.19) and (4.20) and $\beta(\boldsymbol{\mu})$ in Eq. (4.24).

4.4. Offline–online computational procedure and adaptive algorithm

In this Section we discuss the details of the RB numerical solution. We highlight the importance of the offline–online decomposition of the computational procedure for the RB problem and we provide the adaptive algorithm for the choice of the primal and dual sample sets. See also [13, 16, 26].

4.4.1. Numerical issues

The norm $\|\| \cdot \|\|$ of Eqs. (3.11) or (3.21) depends on the parameter $\boldsymbol{\mu} \in \mathcal{D}$; however, for computational reasons, it is convenient to fix a sample $\bar{\boldsymbol{\mu}} \in \mathcal{D}$ for which the norm is evaluated, s.t. the norms (3.11) and (3.21) become respectively:

$$\|\|v\|\|_{\bar{\boldsymbol{\mu}}}^2 := \varepsilon_h(h, \bar{\boldsymbol{\mu}}) \|\nabla v\|^2 + \delta_h(h, \bar{\boldsymbol{\mu}}) \|\mathbf{b}(\bar{\boldsymbol{\mu}}) \cdot \nabla v\|^2 + \|v\|^2, \quad (4.27a)$$

$$\begin{aligned} \|\|v\|\|_{\bar{\boldsymbol{\mu}}}^2 &:= \varepsilon_h(h, \bar{\boldsymbol{\mu}}) \|\nabla v\|^2 + \delta_h(h, \bar{\boldsymbol{\mu}}) \|\mathbf{b}(\bar{\boldsymbol{\mu}}) \cdot \nabla v\|^2 + \|v\|^2 \\ &\quad + \frac{1 + \delta_h(h, \bar{\boldsymbol{\mu}})}{2} \|(\mathbf{b}(\bar{\boldsymbol{\mu}}) \cdot \hat{\mathbf{n}})^{1/2} v\|_{\Gamma_N}^2. \end{aligned} \quad (4.27b)$$

This does not affect the a priori FE and RB error estimates (see, sections 3.2.1, 3.2.2 and 4.2) and the a posteriori RB estimate (see Sec. 4.3): simply, the quantities related to the parametrical “fixed” norm should be recomputed according to $\|\| \cdot \|\|_{\bar{\boldsymbol{\mu}}}$. For example, the inf–sup constant $\beta(\boldsymbol{\mu})$ (4.24), defined w.r.t the “fixed” norm reads:

$$\bar{\beta}(\boldsymbol{\mu}) := \inf_{w_h \in \mathcal{V}_h \setminus \{0\}} \sup_{v_h \in \mathcal{V}_h \setminus \{0\}} \frac{A_h(w_h, v_h; \boldsymbol{\mu})}{\|\|w_h\|\|_{\bar{\boldsymbol{\mu}}} \|\|v_h\|\|_{\bar{\boldsymbol{\mu}}}} \quad \forall \boldsymbol{\mu} \in \mathcal{D}. \quad (4.28)$$

For the evaluation of the a posteriori RB error estimate (4.25), we need the expression of $\bar{\beta}(\boldsymbol{\mu})$ or its lower bound. With this aim, we use a composite linear polynomial interpolator ([22]) defined on the parameter space \mathcal{D} :

$$\tilde{\beta}(\boldsymbol{\mu}) := \sum_{m=1}^K \bar{\beta}(\boldsymbol{\mu}_m) \Pi_m(\boldsymbol{\mu}), \quad (4.29)$$

where $\{\Pi_m(\boldsymbol{\mu})\}_{m=1}^K$ is the basis functions associated with the linear interpolant and $\{\boldsymbol{\mu}_m\}_{m=1}^K$ the samples, chosen in \mathcal{D} , with K the number of samples. The choice of the samples $\{\boldsymbol{\mu}_m\}_{m=1}^K$ and K is made by means of inspection of the function $\bar{\beta}(\boldsymbol{\mu})$ for $\boldsymbol{\mu} \in \mathcal{D}$. We refer the reader to [28] for other possibilities.

From this it follows that the a posteriori RB estimate (4.25) reads now:

$$|s_h(\boldsymbol{\mu}) - \tilde{s}_N(\boldsymbol{\mu})| \leq \bar{\Delta}_N^s(\boldsymbol{\mu}) \quad \forall \boldsymbol{\mu} \in \mathcal{D}. \quad (4.30)$$

where $\bar{\Delta}_N^s(\boldsymbol{\mu}) := \bar{\Delta}_N^{pr}(\boldsymbol{\mu}) \bar{\Delta}_N^{du}(\boldsymbol{\mu})$, with:

$$\bar{\Delta}_N^{pr}(\boldsymbol{\mu}) := \frac{1}{\sqrt{\tilde{\beta}(\boldsymbol{\mu})}} \|\| R_N^{pr}(\cdot; \boldsymbol{\mu}) \|\|_{\bar{\boldsymbol{\mu}}^*}, \quad \bar{\Delta}_N^{du}(\boldsymbol{\mu}) := \frac{1}{\sqrt{\tilde{\beta}(\boldsymbol{\mu})}} \|\| R_N^{du}(\cdot; \boldsymbol{\mu}) \|\|_{\bar{\boldsymbol{\mu}}^*}, \quad (4.31)$$

being $\|\| \cdot \|\|_{\bar{\boldsymbol{\mu}}^*}$ the dual norm associated with $\|\| \cdot \|\|_{\bar{\boldsymbol{\mu}}}$.

The RB problems make use of the parameter $\boldsymbol{\mu}$ chosen in the space \mathcal{D} . However, for computational reasons, the research of the RB sample sets \mathcal{S}_N^{pr} , \mathcal{S}_N^{du} must be restricted to a discrete subset $\bar{\mathcal{D}} \subset \mathcal{D}$ with a number of samples \bar{N} “sufficiently large”. In order to evaluate the RB error, it is convenient to define the following indicators for the maximum and mean output errors for any given N^{pr} and N^{du} :

$$E_N^{max} := \max_{\boldsymbol{\mu} \in \bar{\mathcal{D}}} |s_h(\boldsymbol{\mu}) - \tilde{s}_N(\boldsymbol{\mu})|, \quad E_N^{mean} := \frac{1}{\bar{N}} \left(\sum_{\boldsymbol{\mu} \in \bar{\mathcal{D}}} |s_h(\boldsymbol{\mu}) - \tilde{s}_N(\boldsymbol{\mu})| \right). \quad (4.32)$$

Similarly, in order to evaluate the sharpness of the estimator $\bar{\Delta}_N^s(\boldsymbol{\mu})$, we introduce (see [16]) the *effectivity index*:

$$\bar{\eta}_N^s := \frac{\max_{\boldsymbol{\mu} \in \bar{\mathcal{D}}} \Delta_N^s(\boldsymbol{\mu})}{\max_{\boldsymbol{\mu} \in \bar{\mathcal{D}}} |s_h(\boldsymbol{\mu}) - \tilde{s}_N(\boldsymbol{\mu})|}, \quad (4.33)$$

which should be greater than (or equal to) one ($\bar{\eta}_N^s \geq 1$).

4.4.2. Offline–online computational procedure

The rapid answer of the RB method in a many query input–output context is highlighted if an appropriate offline–online decomposition procedure, led by the affine decomposition hypothesis, is used.

At the *offline* step we define the RB spaces given the sets \mathcal{S}_N^{pr} , \mathcal{S}_N^{du} ; this choice is performed according to the adaptive algorithm (see Sec. 4.4.3). Then we build the RB orthonormal basis $\{\xi_i\}_{i=1}^{N^{pr}}$, $\{\zeta_i\}_{i=1}^{N^{du}}$ by solving the FE primal and dual problems and we assemble the parameter independent RB matrices A_{Nq}^{pr} , A_{Nq}^{du} and vectors \mathbf{F}_{Nq}^{pr} , \mathbf{L}_{Nq}^{pr} , \mathbf{L}_{Nq}^{du} . Finally, we assemble the matrices and vectors for the evaluation of the a posteriori RB error estimate. These operations highlight, in general, relevant computational costs being dependent on the dimension of the FE problems N_h , which is typically “high”.

At the *online* step, for any given $\boldsymbol{\mu} \in \mathcal{D}$, we assemble the parameter dependent RB matrices $A_N^{pr}(\boldsymbol{\mu})$, $A_N^{du}(\boldsymbol{\mu})$ and vectors $\mathbf{F}_N^{pr}(\boldsymbol{\mu})$, $\mathbf{L}_N^{pr}(\boldsymbol{\mu})$, $\mathbf{L}_N^{du}(\boldsymbol{\mu})$, we solve the primal and dual RB problems (4.5) and (4.9), we compute the corrected output $\tilde{s}_N(\boldsymbol{\mu})$ and, if requested, its error bound by means of the a posteriori RB error estimate (4.25). The online RB computational costs can be accounted by taking into account for the number of operations in the following manner (for more details, see, e.g., [13, 16, 18]):

- assembling of the RB matrices and vectors: $\mathcal{O}(Q_h(N^{pr2} + N^{du2}))$;
- solving the primal and dual RB linear systems: $\mathcal{O}(N^{pr3} + N^{du3})$;
- computing the corrected output: $\mathcal{O}(Q_h N^{pr} N^{du})$;
- evaluating the a posteriori RB estimate (if requested): $\mathcal{O}(Q_h^2(N^{pr2} + N^{du2}))$.

In the second step above, the RB matrices are in general full [16, 18]; for this reason, the linear RB systems (4.5) and (4.9) can be conveniently solved by means of direct methods (see, e.g., [22]) which highlight a computational cost of order $\mathcal{O}(\mathcal{N}^3)$, being \mathcal{N} the dimension of the system.

Let us observe that we have indicated only the orders of the dominating costs for each online step. We refer to the total online computational costs by means of the following indicator (which takes into account for the estimated number of operations):

$$\Lambda_N = \Lambda_N(N^{pr}, N^{du}; Q_h) := N^{pr 3} + N^{du 3} + Q_h (N^{pr 2} + N^{du 2}) + Q_h N^{pr} N^{du}, \quad (4.34)$$

which depends on N^{pr} , N^{du} and Q_h ; let us observe that Q_h depends only on the problem under consideration; this implies that, for any given parametrized problem, the online computational cost depends only on the dimension of the RB problem. We choose to not take into account in the indicator Λ_N for the costs associated with the evaluation of the a posteriori RB error estimate; this in view of the adaptive algorithm proposed in the following section.

4.4.3. Adaptive algorithm

We propose an adaptive algorithm for the choice of the primal and dual sample sets \mathcal{S}_N^{pr} , \mathcal{S}_N^{du} (see also [13, 16, 26]). This strategy is based on the minimization of the computational costs (4.34) associated with the online step and on the a posteriori RB error estimate (4.30).

The proposed adaptive algorithm reads:

1. choose a tolerance tol for the absolute error on the RB deflated output $\tilde{s}_N(\boldsymbol{\mu})$ (4.21);
2. choose randomly in $\overline{\mathcal{D}}$ a sample, $\boldsymbol{\mu}_1^{pr}$, for the FE primal problem and another one, $\boldsymbol{\mu}_1^{du}$, for the FE dual one; set $N^{pr} = 1$, $N^{du} = 1$, initialize the sets \mathcal{S}_N^{pr} , \mathcal{S}_N^{du} and build the RB spaces \mathcal{V}_N^{pr} , \mathcal{V}_N^{du} ;
3. evaluate the RB primal and dual error bounds $\overline{\Delta}_N^{pr}(\boldsymbol{\mu})$ and $\overline{\Delta}_N^{du}(\boldsymbol{\mu})$ (see Eq. (4.31)), $\forall \boldsymbol{\mu} \in \overline{\mathcal{D}}$, which requires the solution of the RB primal and dual problems;
4. if $\max_{\boldsymbol{\mu} \in \overline{\mathcal{D}}} \overline{\Delta}_N^{pr}(\boldsymbol{\mu}) < \sqrt{tol}$ or $\max_{\boldsymbol{\mu} \in \overline{\mathcal{D}}} \overline{\Delta}_N^{du}(\boldsymbol{\mu}) < \sqrt{tol}$, jump to step 6, otherwise go to step 5 (in general $N^{pr} \neq N^{du}$ and the "stopping" criterium can be fulfilled separately for the primal and dual problems);
5. set $N^{pr} = N^{pr} + 1$ and $N^{du} = N^{du} + 1$, choose the primal and dual samples as:

$$\boldsymbol{\mu}_{N^{pr}}^{pr} = \operatorname{argmax}_{\boldsymbol{\mu} \in \overline{\mathcal{D}}} \overline{\Delta}_{N^{pr}-1}^{pr}(\boldsymbol{\mu}), \quad \boldsymbol{\mu}_{N^{du}}^{du} = \operatorname{argmax}_{\boldsymbol{\mu} \in \overline{\mathcal{D}}} \overline{\Delta}_{N^{du}-1}^{du}(\boldsymbol{\mu}), \quad (4.35)$$

update the sets \mathcal{S}_N^{pr} , \mathcal{S}_N^{du} and the RB spaces \mathcal{V}_N^{pr} , \mathcal{V}_N^{du} and return to step 3;

6. set $N_{max}^{pr} = N^{pr}$ and $N_{max}^{du} = N^{du}$ and build a matrix (table), let say $D_N \in \mathbb{R}^{N_{max}^{pr} \times N_{max}^{du}}$, whose entries are:

$$(D_N)_{i,j} := \max_{\boldsymbol{\mu} \in \overline{\mathcal{D}}} \left(\overline{\Delta}_i^{pr}(\boldsymbol{\mu}) \overline{\Delta}_j^{du}(\boldsymbol{\mu}) \right) \quad i = 1, \dots, N_{max}^{pr}, \quad j = 1, \dots, N_{max}^{du}; \quad (4.36)$$

7. set a vector of prescribed “error levels”, let say $E_{lev} \in \mathbb{R}^Z$, s.t. $E_{lev} = \{tol_1, \dots, tol_Z\}$, for some $Z \in \mathbb{N}$ and $tol_1 > \dots > tol_Z$, with $tol_Z \leq tol$;
8. for each error level $\{tol_m\}_{m=1}^Z$ identify the entries i_m, j_m of the matrix D_N s.t. $(D_N)_{i_m, j_m} < E_{lev}$; among these, select the coordinates N_m^{pr} and N_m^{du} s.t.:

$$(N_m^{pr}, N_m^{du}) = \underset{i_m, j_m}{\operatorname{argmin}} \Lambda_N(i_m, j_m; Q_h) \quad m = 1, \dots, Z, \quad (4.37)$$

where Λ_N is the indicator of the online computational cost (4.34);

9. build a matrix (table), say E_N , with Z rows and 4 columns in order to summarize the results of the whole procedure; in the first column we report the vector of the error levels E_{lev} , while in the following ones the corresponding number of primal and dual RB basis N_m^{pr} , N_m^{du} and the online computational costs indicator $\Lambda_N(N_m^{pr}, N_m^{du}; Q_h)$, respectively.

Remark 4.3. The proposed adaptive algorithm allows to avoid the computation of the a posteriori RB error estimate (4.30) at the online step: in fact, once we have decided an error level, it is immediate to provide the corresponding maximum error bound and the number of basis for primal and dual RB, simply by accessing the matrix (table) E_N . Moreover, at the offline step, we assemble the RB matrices and vectors A_{Nq}^{pr} , A_{Nq}^{du} , \mathbf{F}_N^{pr} , \mathbf{L}_N^{pr} and \mathbf{L}_N^{du} for N_{max}^{pr} and N_{max}^{du} , which, at the online step for given $N^{pr} < N_{max}^{pr}$ and $N^{du} < N_{max}^{du}$, are obtained simply by eliminating the exceeding rows and columns from the “complete” RB matrices and vectors (the associated online computational costs are negligible w.r.t. other dominating costs).

Remark 4.4. As anticipated in Remark 4.2, we have used the non integrated approach for the choice of the sets \mathcal{S}_N^{pr} and \mathcal{S}_N^{du} . This is the consequence of the adaptive algorithm used: the crucial point is at step 5, where the samples are chosen according to the RB primal and dual error indicators $\bar{\Delta}_N^{pr}(\boldsymbol{\mu})$ and $\bar{\Delta}_N^{du}(\boldsymbol{\mu})$. In fact, even if the primal and dual problems assume the same behavior, they can show very different solutions depending also on the functionals $F_h(\cdot; \boldsymbol{\mu})$ and $L(\cdot; \boldsymbol{\mu})$. Hence, the proposed adaptive algorithm allows to fit the samples as best as possible, both for the primal and dual problems, in view of the computation of the output functional.

5. Combining the Finite Element and Reduced Basis Approximations

In Sections 3 and 4 we have discussed the FE and RB methods for the numerical solution of the parametrized problem of Sec. 2.1. These approaches should not be seen as separate for the solution of our problem, but rather as complementary.

Let us recall that our continuous problem is hyperbolic as shown in Sec. 2.1. For the numerical approximation of this problem we have considered the FE method with stabilization; with this aim, we have provided the stabilized problem in Sec. 3.1 by introducing the stabilized bilinear form $A_h(\cdot, \cdot; \boldsymbol{\mu})$ and functional $F_h(\cdot; \boldsymbol{\mu})$. Let us observe that at this step, we have the following error on the output:

$$|s(\boldsymbol{\mu}) - s_h(\boldsymbol{\mu})| \quad \forall \boldsymbol{\mu} \in \mathcal{D}, \quad (5.1)$$

where $s(\boldsymbol{\mu})$ and $s_h(\boldsymbol{\mu})$ are defined in Eqs. (2.5) and (3.5) (i.e., $\forall \boldsymbol{\mu} \in \mathcal{D}$ we solve a computationally expensive FE problem). As shown by the a priori error estimate (3.20), the error

$$|s(\boldsymbol{\mu}) - s_h(\boldsymbol{\mu})| \rightarrow 0 \text{ as } h \rightarrow 0, \forall \boldsymbol{\mu} \in \mathcal{D}.$$

The RB method is based on the FE approximation (the “truth” one); with this aim, the stabilized Galerkin problem is used in order to define the RB method in Sec. 4. For this reason the RB error on the output is evaluated w.r.t. the FE output for a given parameter $\boldsymbol{\mu} \in \mathcal{D}$, i.e.:

$$|s_h(\boldsymbol{\mu}) - s_N(\boldsymbol{\mu})| \quad \forall \boldsymbol{\mu} \in \mathcal{D}, \quad (5.2)$$

where $s_N(\boldsymbol{\mu})$ is defined in Eq. (4.6). The a priori RB error estimate (4.17) shows that the error $|s_h(\boldsymbol{\mu}) - s_N(\boldsymbol{\mu})| \rightarrow 0$, as N increases ($N \rightarrow \infty$), where N indicates generically the size of the primal and dual RB problems.

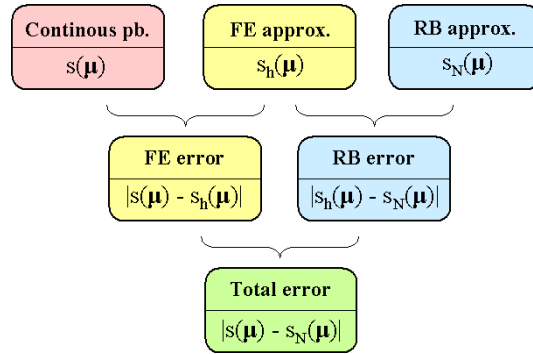


Fig. 5.1. Scheme for numerical solution of the parameterized problem: total, FE and RB errors.

The total error on the output is composed by two terms, given from Eq.s (5.1) and (5.2):

$$|s(\boldsymbol{\mu}) - s_N(\boldsymbol{\mu})| \leq |s(\boldsymbol{\mu}) - s_h(\boldsymbol{\mu})| + |s_h(\boldsymbol{\mu}) - s_N(\boldsymbol{\mu})| \quad \forall \boldsymbol{\mu} \in \mathcal{D}. \quad (5.3)$$

In Fig. 5.1 the previous issues are outlined by means of a block diagram. However, even if $N \rightarrow \infty$ the total error reduces, due to the reduction of the RB part of the error, this is not the case for $h \rightarrow 0$. In fact, by referring e.g. to Problem 1 endowed with the properties of Problem 3, if $h \rightarrow 0$ the FE error reduces according to the a priori FE error estimate (3.20), but the RB error increases for any given N ; this is due to the term $\Xi(\boldsymbol{\mu})$ (4.11) of the a priori RB estimate (4.17), which is of order $h^{-1/2}$. This shows that, for a given $\boldsymbol{\mu} \in \mathcal{D}$ and a fixed N , the RB error could increase as $h \rightarrow 0$; in other words, if the stabilized problem tends to assume a hyperbolic nature (for $h \rightarrow 0$), the “complexity” of the RB problem enhances, i.e. the number of RB basis N should be increased in order to fulfil a prescribed accuracy on the RB error.

For further examples about the RB method for hyperbolic problems, see [15, 29].

6. Numerical Tests

We discuss two numerical tests, referring to the problems outlined in Sections 2.2 and 2.3. Both the tests are inspired by environmental applications concerning with air pollution, for which the goal consists in evaluating the mean concentration of a pollutant in an area of

interest (e.g. a city) emitted by a source (e.g., an industrial chimney) (see, [5, 19, 21]). Such a pollutant is transported by a wind field and can react in air; diffusion processes are considered negligible. Adimensional values are considered for the data and results of the numerical tests.

6.1. Problem 1 (PB1): physical parametrization

Let us consider the Problem 1 of Sec. 2.2. By referring to Eq. (2.8), we consider the domain Ω reported in Fig. 6.1, where we have defined two internal subdomains Ω_{emis} and Ω_{meas} . We assume $\mu_p \in \mathcal{D} = [1, 10^3]$, $\mathbf{V} = \hat{\mathbf{x}}$, $g = \chi_{emis}(\mathbf{x})$ and $\delta = 1/|\Omega_{meas}| \chi_{meas}(\mathbf{x})$, being the unit vector $\hat{\mathbf{x}} := (1, 0) \in \mathbb{R}^2$ and $\mathbf{x} = (x, y) \in \mathbb{R}^2$; $\chi_{emis}(\mathbf{x})$ and $\chi_{meas}(\mathbf{x})$ are the characteristic functions of the subdomains Ω_{emis} and Ω_{meas} , respectively, with $|\Omega_{meas}|$ the area of Ω_{meas} . Then,

$$\Gamma_D = \{\mathbf{x} = (x, y) \in \partial\Omega : x = 0\}$$

as reported in Fig. 6.1. This problem admits an affine decomposition on the bilinear form and functionals: by referring to Sec. 3.1, we have $Q_h = 2$, $Q_h^F = 1$ and $Q^L = 1$ (see Eqs. (3.6) and (2.7)). In order to evaluate the norm $||| \cdot |||$, which depends on μ_p as described in Sec. 4.4.1, we choose $\bar{\mu}_p = 1$; for the sake of simplicity we indicate $||| \cdot |||_{\bar{\mu}_p}$ simply by $||| \cdot |||$.

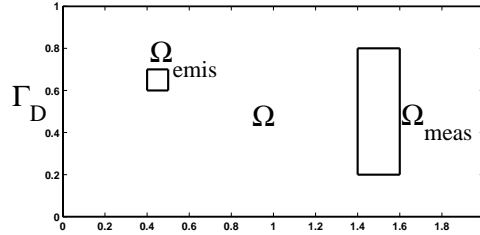


Fig. 6.1. PB1. Domain, subdomains and Dirichlet boundary.

A quasi-uniform mesh with 7,556 triangles ($h = 0.0265$) is used to solve the FE problem. Moreover, we choose (see Eq. (3.3)) $\varepsilon_h = c_\varepsilon \mu_p h^{3/2}$ and $\delta_h = c_\delta h / \mu_p$, where, in order to limit the under and over-shooting of the FE solution $\forall \mu_p \in \mathcal{D}$, we assume $c_\varepsilon = 5 \cdot 10^{-2}$ and $c_\delta = 5 \cdot 10^{-2}$. In Fig. 6.2 we report the solutions of the FE primal problem (concentrations of the pollutant) for the choices $\mu_p = 1$ (left) and $\mu_p = 10^3$ (right); the corresponding FE dual solutions show similar behaviors even if the solutions arise from Ω_{meas} and the flow direction is opposite to that of the primal one. The computed output $s_h(\mu_p)$ corresponds to the FE approximation of the mean concentration in the area Ω_{meas} for some intensity $\mu_p \in \mathcal{D}$ of the wind field.

We solve now the parametrized problem by means of the RB method outlined in Sec.4 and we provide some results concerning with the a priori and a posteriori RB error estimates.

In Fig. 6.3 (left) we compare the a priori RB primal error estimate (4.10) with the true RB error on the primal solution $|||e_N^{pr}(\mu_p)|||$ for different values of $\mu_p \in \mathcal{D}$, being $N^{pr} = 4$ and $\mathcal{S}_N^{pr} = \{1.00, 1.52, 3.06, 93.29\}$. In similar way, in Fig. 6.3 (right) the a priori RB error estimate for the output (4.17) is compared with the RB output error $|s_h(\mu_p) - s_N(\mu_p)|$ for $\mu_p \in \mathcal{D}$; in this case $N^{pr} = N^{du} = 4$, with \mathcal{S}_N^{pr} chosen as previously mentioned and $\mathcal{S}_N^{du} = \{1.00, 1.42, 2.48, 9.33\}$. In order to highlight the effect of the FE mesh on $\Xi(\mu_p)$ (4.15), we compare three quasi-uniform meshes with 2,680, 7,556 and 17,016 triangles, thus observing that e.g. for $\mu_p = 10^2$, we obtain $\Xi(\mu_p) \simeq 205, 280$ and 325 respectively. In general, as h decreases (i.e., the FE solution

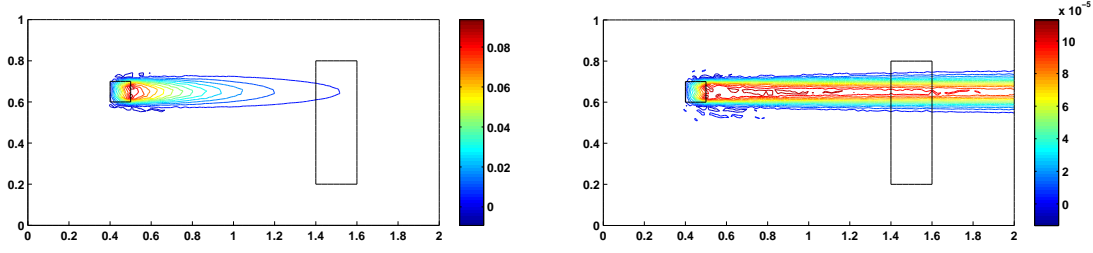


Fig. 6.2. PB1. FE primal solutions (concentration of the pollutant, adimensional values) for $\mu_p = 1$ (left) and $\mu_p = 10^3$ (right).

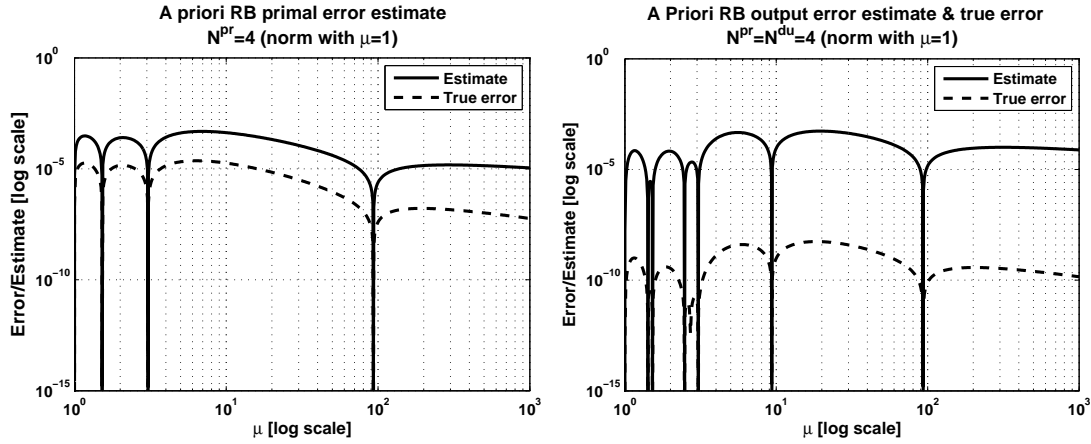


Fig. 6.3. PB1. A priori RB error estimates (continuous) and true RB errors (dashed) vs $\mu_p \in \mathcal{D}$: RB primal error for $N^{pr} = 4$ (left) and RB output error for $N^{pr} = N^{du} = 4$ (right); logarithmic scales on both axis.

“improves”), then the parametrized constant $\Xi(\mu_p)$ increases for any fixed values of $\mu_p \in \mathcal{D}$, thus affecting the sharpness property of the a priori RB estimates (4.10), (4.18) and (4.17).

We deal now with the a posteriori RB error estimate (4.25) (and (4.30)) used in the adaptive algorithm of Sec.4.4.3 for the choice of the RB samples and basis. Firstly, we need to evaluate the parametrized inf–sup stability constant $\beta(\mu_p)$ (4.24); with this aim, we use the numerical procedure outlined in Sec. 4.4.1 (Eqs. (4.28) and (4.29)). Being $\mathcal{D} \subset \mathbb{R}$, we choose for $\{\Pi_m(\mu_p)\}_{m=1}^K$ a polynomial approximation in the least–squares sense of degree 3 obtained by means of the logarithmic–equally spaced pairs $(\mu_{p,m}, \bar{\beta}(\mu_{p,m}))$, $m = 1, \dots, K$ with $K = 9$. In Fig. 6.4 we compare the a posteriori RB error estimator for the output (4.30) and the RB error for $N^{pr} = N^{du} = 4$; the sample sets \mathcal{S}_N^{pr} and \mathcal{S}_N^{du} are the same chosen for the results of Fig. 6.3 (left) and (right).

The a posteriori RB error estimator (4.30) is used in the adaptive algorithm proposed in Sec. 4.4.3 for the choice of \mathcal{S}_N^{pr} and \mathcal{S}_N^{du} . The results of the adaptive algorithm are summarized in Table 6.1 by means of the matrix (table) E_N defined at point 9 of Sec. 4.4.3; in order to show the effectivity of the “primal–dual” RB approach we compare the results with those of an “only primal” RB approach, highlighting the savings of computational costs allowed by

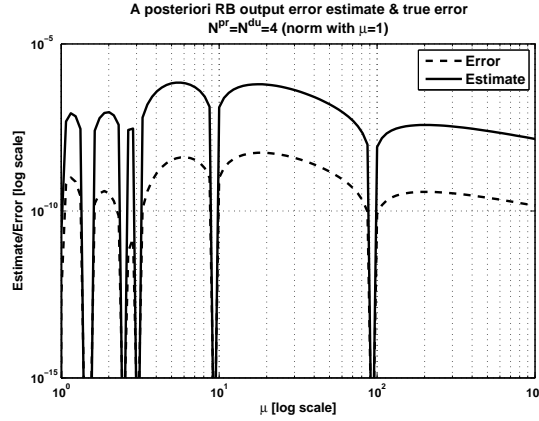


Fig. 6.4. PB1. A posteriori RB error estimate for the output (4.30) with $N^{pr} = N^{du} = 4$ (continuous) and RB error (dashed) vs $\mu_p \in \mathcal{D}$; logarithmic scales on both axis.

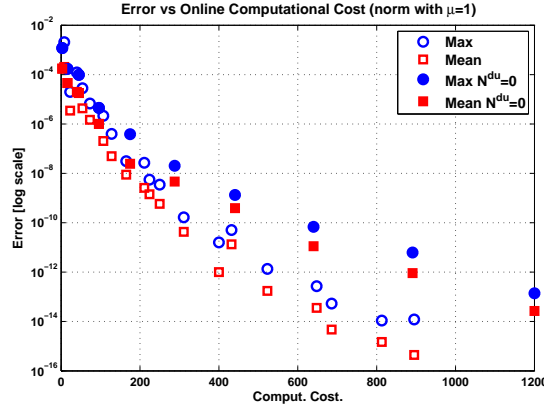


Fig. 6.5. PB1. E_N^{max} (empty circle) and E_N^{mean} (empty square) for the “primal–dual” RB approach vs online computational costs $\Lambda_N^{pr,du}$, Λ_N^{pr} (estimated number of operations); full circles and squares refer to the indicators E_N^{max} , E_N^{mean} for the “only primal” RB approach. Error axis in logarithmic scale.

the former one. In Table 6.1 we report, for some error levels E_{lev} on the output, the selected number of basis N^{pr} , N^{du} and the online computational costs (estimated number of operations) associated with the “primal–dual” ($\Lambda_N^{pr,du} = \Lambda_N$, see Eq. (4.34)) and the “only primal” (Λ_N^{pr}) RB approaches respectively; moreover, we report the ratio $\Lambda_N^{pr}/\Lambda_N^{pr,du}$ for each error level. Let us notice that in the case for which $N^{pr} > 0$ and $N^{du} = 0$, the “primal–dual” RB approach is equivalent to the “only primal” one. As we can also observe from Table 6.1, we always have $\Lambda_N^{pr} \geq \Lambda_N^{pr,du} \forall E_{lev}$; this shows the effectiveness of the “primal–dual” RB approach w.r.t. the “only primal” one, which is more expensive already for this simple test problem with a single parameter μ_p . For example, if we require an error level $E_{lev} = 10^{-8}$ (which for this problem yields a relative error on $s(\mu_p)$ inferior than 0.1% $\forall \mu_p \in \mathcal{D}$) the “primal–dual” RB approach selects $N^{pr} = N^{du} = 5$ w.r.t. $N^{pr} = 8$ requested by the “only primal” RB approach and it allows a saving of the online computational costs of 1.6 times. We notice that even larger computational costs savings can be obtained; e.g. for $E_{lev} = 1.778 \cdot 10^{-10}$, the saving is about of 2.3 times. Let us observe that the adaptive algorithm does not tend to select the case $N^{du} = 0$

Table 6.1: PB1. Adaptive algorithm: results and comparison between the ‘primal–dual’ and the ‘only primal’ RB approach for some error levels E_{lev} .

E_{lev}	“primal–dual” RB			“only primal” RB		$\Lambda_N^{pr}/\Lambda_N^{pr,du}$
	N^{pr}	N^{du}	$\Lambda_N^{pr,du}$	N^{pr}	Λ_N^{pr}	
$1.000e-01$	1	0	$3.000e+00$	1	$3.000e+00$	1.000
$5.623e-02$	1	1	$8.000e+00$	2	$1.600e+01$	2.000
$3.162e-02$	2	0	$1.600e+01$	2	$1.600e+01$	1.000
$1.778e-02$	1	2	$2.300e+01$	3	$4.500e+01$	1.957
$1.000e-02$	2	2	$4.000e+01$	3	$4.500e+01$	1.125
$3.162e-03$	3	0	$4.500e+01$	3	$4.500e+01$	1.000
$1.778e-03$	1	3	$5.400e+01$	4	$9.600e+01$	1.778
$5.623e-04$	2	3	$7.300e+01$	4	$9.600e+01$	1.315
$3.162e-04$	4	0	$9.600e+01$	4	$9.600e+01$	1.000
$1.000e-04$	4	1	$1.070e+02$	5	$1.750e+02$	1.636
$5.623e-05$	4	2	$1.280e+02$	5	$1.750e+02$	1.367
$3.162e-05$	4	3	$1.650e+02$	5	$1.750e+02$	1.061
$5.623e-06$	4	3	$1.650e+02$	6	$2.880e+02$	1.745
$3.162e-06$	5	2	$2.110e+02$	6	$2.880e+02$	1.365
$1.000e-06$	4	4	$2.240e+02$	6	$2.880e+02$	1.286
$5.623e-07$	3	5	$2.500e+02$	7	$4.410e+02$	1.764
$5.623e-08$	5	4	$3.110e+02$	7	$4.410e+02$	1.418
$1.778e-08$	5	4	$3.110e+02$	8	$6.400e+02$	2.058
$1.000e-08$	5	5	$4.000e+02$	8	$6.400e+02$	1.600
$5.623e-09$	5	5	$4.000e+02$	9	$8.910e+02$	2.228
$3.162e-09$	6	4	$4.320e+02$	9	$8.910e+02$	2.062
$5.623e-10$	6	5	$5.230e+02$	9	$8.910e+02$	1.704
$1.778e-10$	6	5	$5.230e+02$	10	$1.200e+03$	2.294
$1.000e-10$	6	6	$6.480e+02$	10	$1.200e+03$	1.852

as E_{lev} decreases.

Finally, we compare the RB output errors obtained by means of the adaptive algorithm for the “primal–dual” RB approach with those of the “only primal” one; with this aim, we use the RB error indicators E_N^{max} and E_N^{mean} (see Eq. (4.32)). In Fig. 6.5 we report E_N^{max} and E_N^{mean} vs the online computational cost $\Lambda_N^{pr,du}$ and Λ_N^{pr} for both the “primal–dual” and “only primal” RB approaches. The plot shows that the “primal–dual” RB approach allows to minimize the online computational costs for any given error tolerance on the output; for example, if we fix the tolerance error at 10^{-12} we see that $\Lambda_N^{pr,du}$ is about the half of Λ_N^{pr} . This confirms, a posteriori, the validity of the adaptive algorithm and the criterium of the “minimum online computational costs”. Finally, we observe that the effectivity index indicators $\bar{\eta}_N^s \in [20, 700]$ (see Eq. (4.33)) for both the RB approaches, with no particular differences.

6.2. Problem 2 (PB2): physical and geometrical parametrization

By considering now the Problem 2 of Sec. 2.3, we introduce the geometrical parameter, μ_g s.t. the real domain Ω_0 could be affinely mapped into a reference one Ω . In Fig. 6.6 (left) we report the real domain Ω_0 , which is partitioned into 5 subdomains Ω_{0i} , s.t. $\cup_{i=1}^5 \Omega_{0i} = \Omega_0$. The

geometrical parameter μ_g (with signum) measures the distance between the mid abscissa of the subdomain Ω_{03} and the line $x_0 = 0$; the subdomains Ω_{01} and Ω_{05} are fixed, while Ω_{02} and Ω_{04} deform in affine manner according to the moving of Ω_{03} . All the subdomains Ω_{0i} can be mapped in Ω by means of affine maps in the form (2.11); the reference domain $\Omega = \cup_{i=1}^5 \Omega_i$ is reported in Fig. 6.6 (right). The subdomains Ω_{emis} and Ω_{meas} are fixed w.r.t. the subdomains Ω_{03} and Ω_{05} , respectively; the Dirichlet boundary corresponds to the upper boundary of Ω .

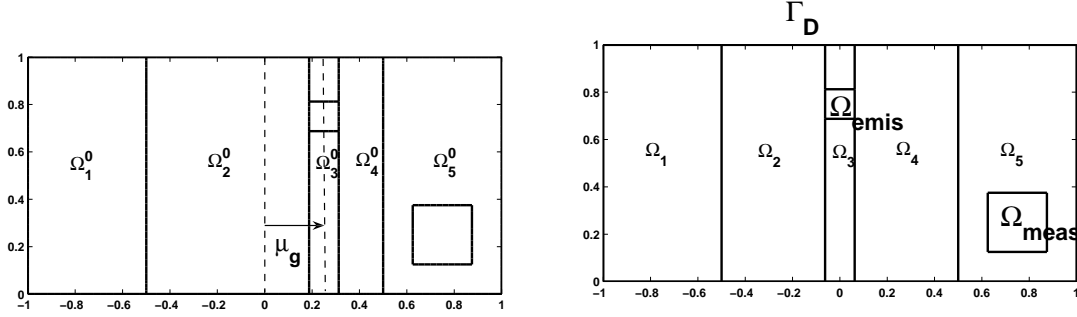


Fig. 6.6. PB2. Real Ω_0 (left) and reference Ω (right) domains; geometrical parameter and Dirichlet boundary.

The parameter vector is $\boldsymbol{\mu} = (\mu_g, \mu_p) \in \mathcal{D} = [\mu_g^{min}, \mu_g^{max}] \times [\mu_p^{min}, \mu_p^{max}]$, where, in order to avoid the degeneration of the subdomains Ω_{02} and Ω_{04} , we choose $\mu_g^{min} = -3/8$, $\mu_g^{max} = 3/8$; then, $\mu_p^{min} = 1$ and $\mu_p^{max} = 10^3$. Moreover, by recalling the notation of Sections 2.3 and 6.1, we choose

$$\mathbf{V}_0 = x_0 \hat{\mathbf{x}} - y_0 \hat{\mathbf{y}}, g_0 = \chi_{meas}(\mathbf{x}_0) \quad \text{and} \quad \delta_0 = 1/|\Omega_{meas}| \chi_{meas}(\mathbf{x}_0),$$

where $\mathbf{x}_0 = (x_0, y_0) \in \mathbb{R}^2$. By considering the data reported on the reference domain (see Eq. (2.12)), we obtain the problem in the general weak form (2.2). It is simple to show that, for the problem under consideration, the hypothesis on the data requested in Sec. 2.1 are satisfied; in particular, the property $\nabla \cdot \mathbf{b}(\boldsymbol{\mu}) = 0 \quad \forall \boldsymbol{\mu} \in \mathcal{D}$ holds. The weak problem admits an affine decomposition for which we have $Q_h = 16$, $Q_h^F = 2$ and $Q^L = 1$ (see Eqs. (3.3) and (2.7)). As reported in Sec.4.4.1, for the evaluation of the norm $||| \cdot |||$ we choose $\bar{\boldsymbol{\mu}} = (\bar{\mu}_g, \bar{\mu}_p) = (0, 1)$.

For the FE solution of the problem we choose a quasi-uniform mesh for the reference domain Ω with 7,504 triangles and the constants (3.3) as $\varepsilon_h(h, \mu_p) = c_\varepsilon \mu_p h^{3/2}$ and $\delta_h = c_\delta h / \mu_p$ with $c_\varepsilon = 2 \cdot 10^{-1}$ and $c_\delta = 2 \cdot 10^{-1}$. In Fig. 6.7 we report the primal FE solutions (concentrations of the pollutant), mapped from Ω into Ω_0 , for different choices of $\boldsymbol{\mu} \in \mathcal{D}$. As shown, the primal solution strongly depends on the values assumed by the geometrical parameter μ_g and not only by the physical one μ_p . On the contrary, for this particular problem, the behavior of the dual solution in the real domain Ω_0 is not influenced by the geometrical parameter, being the “dual source” subdomain Ω_{meas} fixed. However, this is not true in the reference domain Ω , being the weak form of the stabilized dual problem (3.9) depending on μ_g .

We solve the parametrized problem by means of the RB method and we discuss the results about the adaptive algorithm and the a posteriori RB estimate; we remark that the output $s_N(\boldsymbol{\mu})$ assumes its maximum values for about $\boldsymbol{\mu} = (0.28, 3.0)$ as it can be seen e.g. by solving the problem by means the “primal-dual” RB approach with $N^{Pr} = 26$ and $N^{du} = 45$ and also

with the “only primal” RB one with $N^{pr} = 120$.

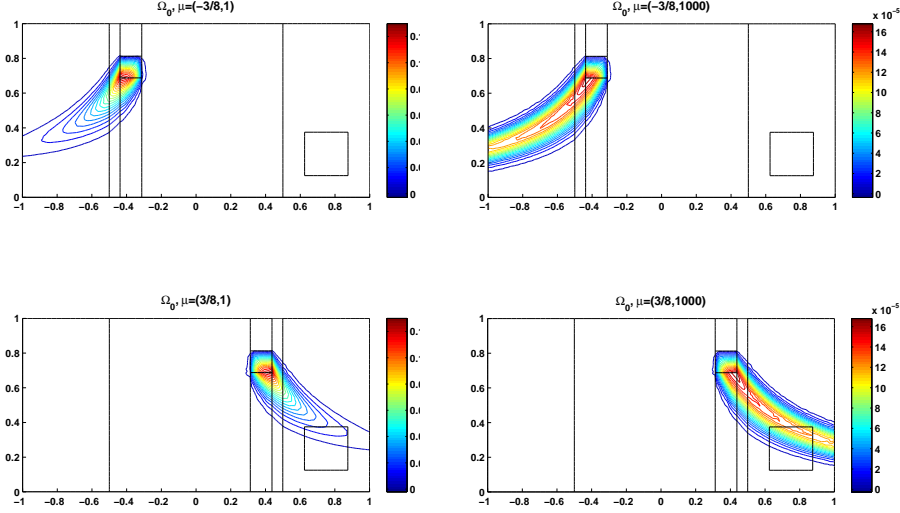


Fig. 6.7. PB2. Primal FE solutions (concentration of the pollutant, adimensional values) in the real domain Ω_0 for $\boldsymbol{\mu} = (-3/8, 1)$ (top-left), $\boldsymbol{\mu} = (-3/8, 10^3)$ (top-right), $\boldsymbol{\mu} = (3/8, 1)$ (bottom-left) and $\boldsymbol{\mu} = (3/8, 10^3)$ (bottom-right).

Numerical tests reveal the validity of the a priori RB error estimates (4.10) and (4.17) also for the problem currently under consideration.

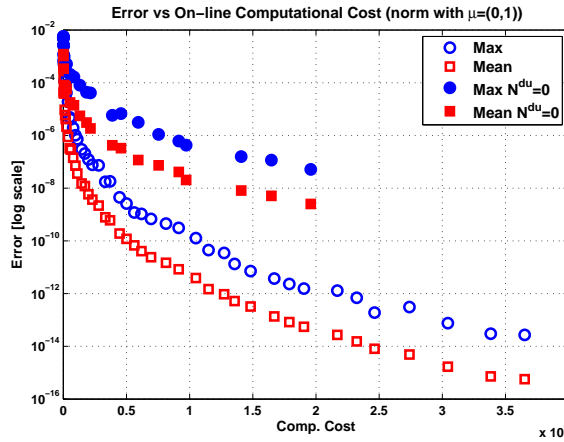
We deal now with the a posteriori RB error estimate for the output (4.25) (and (4.30)) and the adaptive algorithm for the samples selection (see Sec. 4.4.3). In order to use the estimate (4.30), we need to evaluate the inf-sup constant; with this aim, we adopt the procedure of Sec. 4.4.1 obtaining the parametrized constant $\tilde{\beta}(\boldsymbol{\mu})$ (4.29), with $K = 195$.

The a posteriori RB error estimate (4.30) is used in the adaptive algorithm in order to define the sets \mathcal{S}_N^{pr} and \mathcal{S}_N^{du} . The results are reported in Table 6.2 for some error levels E_{lev} by using the matrix E_N (see point 9 of Sec. 4.4.3); the same notation of Table 6.1 is used for Table 6.2. Once again, we observe that $\Lambda_N^{pr} \geq \Lambda_N^{pr,du} \forall E_{lev}$. For example, if we fix $E_{lev} = 10^{-5}$, we see from Table 6.2 that the “primal–dual” RB approach selects $N^{pr} = 27$ and $N^{du} = 41$ w.r.t. $N^{pr} = 113$ chosen by the “only primal” one; more over, the saving of online computational cost is considerable, being of about 11 times inferior. Even larger savings are allowed for the problem under consideration: for example, if $E_{lev} = 5.623 \cdot 10^{-4}$ we have $\Lambda_N^{pr}/\Lambda_N^{pr,du} = 15.687$.

We compare the RB errors on the output obtained on the basis of the adaptive algorithm for the “primal–dual” and the “only primal” RB approaches. In Fig. 6.8 we report the error indicators E_N^{max} and E_N^{mean} (see Eq. (4.32)) vs the online computational costs $\Lambda_N^{pr,du}$ and Λ_N^{pr} (estimated number of operations) for both the “primal–dual” and “only primal” RB approaches. The plot clearly shows that the “primal–dual” RB approach allows great savings of online computational costs for any given error tolerance on the output; for example, if we fix the tolerance error at 10^{-8} we see that $\Lambda_N^{pr,du}$ is about 8 times inferior than Λ_N^{pr} . This confirms the validity of the adaptive algorithm and the indications given in Table 6.2. Finally, the effectivity index indicator $\bar{\eta}_N^s \in [10, 100]$ (see Eq. (4.33)) for both the approaches.

Table 6.2: PB2. Adaptive algorithm: results of samples selection procedure and comparison between the ‘primal–dual’ and the ‘only primal’ RB approach for some error levels E_{lev} .

E_{lev}	“primal–dual” RB			“only primal” RB		$\Lambda_N^{pr}/\Lambda_N^{pr,du}$
	N^{pr}	N^{du}	$\Lambda_N^{pr,du}$	N^{pr}	Λ_N^{pr}	
$5.623e-01$	1	0	$1.700e+01$	1	$1.700e+01$	1.000
$3.162e-01$	2	2	$2.080e+02$	4	$3.200e+02$	1.538
$1.778e-01$	4	0	$3.200e+02$	4	$3.200e+02$	1.000
$1.000e-01$	1	5	$6.220e+02$	11	$3.267e+03$	5.252
$5.623e-02$	1	6	$9.050e+02$	15	$6.975e+03$	7.707
$3.162e-02$	7	5	$2.212e+03$	22	$1.839e+04$	8.315
$1.778e-02$	7	7	$3.038e+03$	25	$2.562e+04$	8.435
$1.000e-02$	5	11	$4.672e+03$	33	$5.336e+04$	11.421
$5.623e-03$	7	12	$6.503e+03$	39	$8.366e+04$	12.864
$3.162e-03$	5	17	$1.142e+04$	46	$1.312e+05$	11.486
$1.778e-03$	10	17	$1.486e+04$	52	$1.839e+05$	12.376
$1.000e-03$	14	17	$1.922e+04$	55	$2.148e+05$	11.172
$5.623e-04$	14	20	$2.476e+04$	68	$3.884e+05$	15.687
$3.162e-04$	20	21	$3.744e+04$	72	$4.562e+05$	12.186
$1.778e-04$	14	29	$5.022e+04$	79	$5.929e+05$	11.806
$1.000e-04$	21	28	$6.022e+04$	86	$7.544e+05$	12.527
$5.623e-05$	20	33	$7.832e+04$	92	$9.141e+05$	11.671
$3.162e-05$	26	33	$9.548e+04$	94	$9.720e+05$	10.180
$1.778e-05$	29	34	$1.114e+05$	107	$1.408e+06$	12.639
$1.000e-05$	27	41	$1.449e+05$	113	$1.647e+06$	11.370
$5.623e-06$	26	45	$1.706e+05$	120	$1.958e+06$	11.477

Fig. 6.8. PB2. E_N^{max} (empty circle) and E_N^{mean} (empty square) for the “primal–dual” RB approach vs online computational costs $\Lambda_N^{pr,du}$, Λ_N^{pr} (estimated number of operations); full circles and squares refer to the indicators E_N^{max} , E_N^{mean} for the “only primal” RB approach. Error axis in logarithmic scale.

7. Conclusions

In this work we have considered the RB method for the approximation of parametrized advection–reaction PDEs. We have generated the basis by means of the FE method applied

to the stabilized version of the weak problem. For the RB method in the “primal–dual” formulation, we have provided and discussed a priori RB error estimates. We have shown that the RB “complexity” increases as the FE mesh size reduces, thus requiring a larger number of basis in order to satisfy a prescribed tolerance on the error. An adaptive algorithm for the selection of the sample sets, led by the a posteriori RB error estimate and based on a criterium of minimization of the online computational costs, has been elaborated. We have proved, by means of numerical tests, the effectiveness of this algorithm and the savings of computational costs allowed at the online step by the “primal–dual” RB approach w.r.t. those of the “only primal” one. The numerical tests also show that if the FE approximation is stable, then so it is the RB one. In fact, no numerical instabilities incur in the RB solutions once the FE formulation is properly stabilized (in this case by means of the Streamline Diffusion method).

Acknowledgments. The author acknowledges the support provided thorough the “Progetto Rocca”, MIT–Politecnico di Milano collaboration. Many thanks to Prof. A.T. Patera for having introduced me to the world of the Reduced Basis method and welcomed in his group at MIT. Special thanks to Dr. G. Rozza for the suggestions and ideas and to Dr. G.S.H. Pau, Dr. S. Sen and D. Blanchard for the helpful discussions. Many thanks to Prof. A. Quarteroni for the interest, research guidelines and for having encouraged this initiative. Acknowledgements to Dr. S. Sferza and Prof. F. Gazzola for the kind help.

References

- [1] B.O. Almroth, P. Stern, F.A. Brogan, Automatic choice of global shape functions in structural analysis, *AIAA J.*, **16** (1978), 525-528.
- [2] I. Babuška, Error–bounds for finite element method, *Numer. Math.*, **16** (1971), 322-333.
- [3] É. Cancès, C. Le Bris, Y. Maday, N.C. Nguyen, A.T. Patera, G.S.H. Pau, Feasibility and competitiveness of a reduced basis approach for rapid electronic structure calculations in quantum chemistry, *High dimensional partial differential equations in science and engineering, CRM, Proceedings and Lecture Notes*, **41**, Amer. Math. Soc., Providence RI, 2007, 15-47.
- [4] L. Dedè, Adaptive and reduced basis methods for optimal control problems in environmental applications, PhD Thesis, Politecnico di Milano, 2008. <http://mox.polimi.it>
- [5] L. Dedè, A. Quarteroni, Optimal control and numerical adaptivity for advection–diffusion equations, *Math. Model. Numer. Anal.*, **39**:5 (2005), 1019-1040.
- [6] M.A. Grepl, A.T. Patera, A posteriori error bounds for reduced–basis approximations of parametrized parabolic partial differential equations, *Math. Model. Numer. Anal.*, **39**:1 (2005), 157-181.
- [7] D.B.P. Huynh, A.T. Patera, Reduced basis approximation and a posteriori error estimation from stress intensity factors, *Int. J. Numer. Meth. Eng.*, **72**:10 (2007), 1219-1259.
- [8] C. Johnson, Numerical Solution of Partial Differential Equations by the Finite Element Method, Cambridge University Press, Cambridge, 1987.
- [9] C. Johnson, A.H. Schatz, L.B. Wahlbin, Crosswind smear and pointwise errors in streamline diffusion finite element methods, *Math. Comput.*, **49**:179 (1987), 25-38.
- [10] J.L. Lions, E. Magenes, Non–homogeneous Boundary Value Problems and Applications, Vol.I., Springer–Verlag, New York and Heidelberg, 1972.
- [11] A.E. Løvgrén, Y. Maday, E. Rønquist, A reduced basis element method for the steady Stokes problem, *Math. Model. Numer. Anal.*, **40**:3 (2006), 529-552.
- [12] R. Milani, A. Quarteroni, G. Rozza, Reduced basis method for linear elasticity problems with many parameters, *Comput. Method. Appl. M.*, **197**:51-52 (2008), 4812-4829.

- [13] N.C. Nguyen, K. Veroy, A.T. Patera, Certified real-time solution of parametrized partial differential equations, in *Handbook of Materials Modeling*, S. Yip (ed.), Springer, 2005, 1523-1558.
- [14] A.K. Noor, J.M. Peters, Reduced basis technique for nonlinear analysis of structures, *AIAA J.*, **19** (1980), 455-462.
- [15] A.T. Patera, E. Rønquist, Reduced basis approximations and a posteriori error estimation for a Boltzmann model, *Comput. Method. Appl. M.*, **196**:29-30 (2007), 2925-2942.
- [16] A.T. Patera, G. Rozza, Reduced Basis Approximation and A Posteriori Error Estimation for Parametrized Partial Differential Equations, Version 1.0, Copyright MIT 2006-08, to appear in (tentative rubric) MIT Pappalardo Graduate Monographs in Mechanical Engineering, <http://augustine.mit.edu/>
- [17] T.A. Porsching, Estimation of the error in the reduced basis method solution of nonlinear equations, *Math. Comput.*, **45**:172 (1985), 487-496.
- [18] C. Prud'homme, D. Rovas, K. Veroy, Y. Maday, A.T. Patera, G. Turinici, Reliable real-time solution of parametrized partial differential equations: reduced-basis output bound methods, *J. Fluids Eng.*, **124**:1 (2002), 70-80.
- [19] A. Quarteroni, A. Quaini, G. Rozza, Reduced basis methods for advection-diffusion optimal control problems, in *Advances in Numerical Mathematics*, W. Fitzgibbon, R. Hoppe, J. Periaux, O. Pironneau and Y. Vassilevski (ed.s), Moscow, Russian Academy of Science and Houston, University of Houston, 2006, 193-216.
- [20] A. Quarteroni, G. Rozza, Numerical solutions of parametrized Navier-Stokes equations by reduced basis method, *Numer. Meth. Part. Diff. Eqn.*, **23**:4 (2007), 923-948.
- [21] A. Quarteroni, G. Rozza, L. Dedè, A. Quaini, Numerical approximation of a control problem for advection-diffusion processes, in *System modeling and optimization, IFIP Int. Fed. Inf. Process.*, **199**, Springer, New York, 2006, pp. 261-273.
- [22] A. Quarteroni, R. Sacco, F. Saleri, Numerical Mathematics, Springer-Verlag, Berlin, 2007.
- [23] A. Quarteroni, A. Valli, Numerical Approximation of Partial Differential Equations, Springer, Berlin and Heidelberg, 1994.
- [24] G. Rozza, Reduced-basis methods for elliptic equations in sub-domains with a posteriori error bounds and adaptivity, *Appl. Numer. Math.*, **55**:4 (2005), 403-424.
- [25] G. Rozza, Reduced basis methods for Stokes equations in domains with non affine parameter dependence, *Comput. Vis. Sci.*, **12**:1 (2009), 23-35.
- [26] G. Rozza, D.B.P. Huynh, A.T. Patera, Reduced basis approximation and a posteriori error estimation for affinely parametrized elliptic coercive partial differential equations: application to transport and continuum mechanics, *Arch. Comput. Method. E.*, **15**:3 (2008), 229-275.
- [27] G. Rozza, K. Veroy, On the stability of the reduced basis method for Stokes equations in parametrized domains, *Comput. Method. Appl. M.*, **196**:7 (2007), 1244-1260.
- [28] S. Sen, K. Veroy, D.B.P. Huynh, S. Deparis, N.C. Nguyen, A.T. Patera, "Natural norm" a posteriori error estimators for reduced basis approximations, *J. Comput. Phys.*, **217**:1 (2006), 37-62.
- [29] A. Tan Yong Kwang, Reduced Basis Method for 2nd Order Wave Equation: Application to One-Dimension Seismic Problem, Master Thesis, Singapore-MIT Alliance, National University of Singapore, 2006. <http://augustine.mit.edu/>
- [30] K. Veroy, A.T. Patera, Certified real-time solution of the parametrized steady incompressible Navier-Stokes equations: rigorous reduced-basis a posteriori error bounds, *Int. J. Numer. Method. Fl.*, **47** (2005), 773-788.
- [31] G. Zhou. How accurate is the streamline diffusion finite element method? *Math. Comput.*, **66**:217 (1997), 31-44.